© 2019. Published by The Company of Biologists Ltd | Development (2019) 146, dev159343. doi:10.1242/dev.159343

RESEARCH ARTICLE

Wnt produced by stretched roof-plate cells is required for the promotion of cell proliferation around the central canal of the spinal cord

Takuma Shinozuka[1,2,3], Ritsuko Takada[1,2], Shosei Yoshida[2,3], Shigenobu Yonemura[4,5] and Shinji Takada[1,2,3,*]

ABSTRACT

Cell morphology changes dynamically during embryogenesis, and these changes create new interactions with surrounding cells, some of which are presumably mediated by intercellular signaling. However, the effects of morphological changes on intercellular signaling remain to be fully elucidated. In this study, we examined the effect of morphological changes in Wnt-producing cells on intercellular signaling in the spinal cord. After mid-gestation, roof-plate cells stretched along the dorsoventral axis in the mouse spinal cord, resulting in new contact at their tips with the ependymal cells that surround the central canal. Wnt1 and Wnt3a were produced by the stretched roof-plate cells and delivered to the cell process tip. Whereas Wnt signaling was activated in developing ependymal cells, Wnt activation in dorsal ependymal cells, which were close to the stretched roof plate, was significantly suppressed in embryos with roof plate-specific conditional knockout of *Wls*, which encodes a factor that is essential for Wnt secretion. Furthermore, proliferation of these cells was impaired in *Wls* conditional knockout mice during development and after induced spinal cord injury in adults. Therefore, morphological changes in Wnt-producing cells appear to generate new Wnt signal targets.

KEY WORDS: Wnt, Morphogen, Spinal cord, Roof plate, Neural stem cell, Regeneration, Mouse

INTRODUCTION

During embryogenesis and homeostasis, secreted signaling proteins such as Wnts and BMPs regulate cell proliferation and differentiation in a spatially coordinated manner. How physiological changes regulate the activity ranges of these signaling proteins remains to be determined, however. In general, secreted signaling proteins diffuse into the extracellular space, creating a concentration gradient around the producing cells. During morphogenesis, cells dynamically change their shape. Marked changes in the morphology of signal-producing cells during tissue morphogenesis presumably result in the activation of signaling in neighboring cells. However, it is unclear whether changes in cell morphology during tissue morphogenesis actually create new signaling targets.

The developing spinal cord has been thoroughly characterized as a model system for research that is aimed at understanding the spatial regulation of secreted signaling proteins. During early development of the vertebrate spinal cord, the most dorsal region, known as the roof plate, functions as an organizing center by secreting Wnt and BMP (Chizhikov and Millen, 2004; Lee and Jessell, 1999). Several researchers have hypothesized that concentration gradients of these signaling proteins generate patterns of interneuron subtypes in the dorsal spinal cord (Chizhikov and Millen, 2005; Lee et al., 2000; Muroyama et al., 2002). Interestingly, as this patterning event nears completion, the morphology of the spinal cord changes dynamically; that is, the neural tube lumen gradually shrinks and a median septum forms along the dorsoventral axis (Böhme, 1988). A recent study in zebrafish embryos revealed that the roof plate stretches during this morphological change (Kondrychyn et al., 2013). This finding prompted us to ask whether the processes of these stretched roof-plate cells are involved in intercellular communication and whether stretching of roof-plate cells induces changes in those cells that respond to signals from the roof plate.

In adult mice, neural progenitor/stem cells localize around the shrunken lumen of the spinal cord (Hamilton et al., 2009; Johansson et al., 1999; Meletis et al., 2008; Weiss et al., 1996), and this area is referred to as the central canal. The central canal is connected to the ventricle, in which neural progenitor/stem cells localize in the forebrain (Lois and Alvarez-buylla, 1993; Morshead et al., 1994; Weiss et al., 1996). As the proliferation of neural progenitor/stem cells in the brain is regulated by secreted signaling molecules, including Wnt (Adachi et al., 2007; Chenn and Walsh, 2002; Hirabayashi et al., 2004; Kuwabara et al., 2009; Lie et al., 2005; Machon et al., 2007; Munji et al., 2011; Toledo et al., 2008; Varela-Nallar and Inestrosa, 2013; Wrobel et al., 2007), it is plausible that spinal cord progenitor/stem cells are regulated in a similar manner. For better understanding of this regulation, the sources of these signals should be clarified. One intriguing possibility is that stretched roof-plate cells are a source of signaling molecules that target the neural progenitor/stem cells that surround the central canal.

Wnt1 and *Wnt3a* are specifically expressed in the roof plate (Parr et al., 1993) and they play numerous roles in the developing spinal cord, including regulating the proliferation and specification of dorsal interneurons (Muroyama et al., 2002) before the mid-gestation stage. However, owing to poor resolution of current digoxigenin-based *in situ* hybridization methods, whether *Wnt* expression is maintained in stretched roof-plate cells remains unclear. Furthermore, genetic studies of *Wnt1*- and *Wnt3a*-deficient mutant mouse embryos yielded no information regarding the

[1]Exploratory Research Center on Life and Living Systems, National Institutes of Natural Sciences, 5-1 Higashiyama, Myodaiji, Okazaki, Aichi 444-8787, Japan. [2]National Institute for Basic Biology, National Institutes of Natural Sciences, 5-1 Higashiyama, Myodaiji, Okazaki, Aichi 444-8787, Japan. [3]Department of Basic Biology in the School of Life Science, The Graduate University for Advanced Studies (SOKENDAI), 5-1 Higashiyama, Myodaiji, Okazaki, Aichi 444-8787, Japan. [4]RIKEN Center for Life Science Technologies, 2-2-3 Minatojima-minamimachi, Chuo-ku, Kobe, Hyogo 650-0047, Japan. [5]Department of Cell Biology, Tokushima University Graduate School of Medical Science, 3-18-15, Kuramoto-cho, Tokushima 770-8503, Japan.

*Author for correspondence (stakada@nibb.ac.jp)

R.T., 0000-0002-1615-056X; S.Yoshida, 0000-0001-8861-1866; S.T., 0000-0003-4125-6056

Received 11 September 2017; Accepted 14 December 2018

Development (2019) 146, dev159343. doi:10.1242/dev.159343

roles of the respective proteins in later stages, as neither *Wnt1*- nor *Wnt3a*-deficient single mutants exhibit a roof plate-related phenotype, and most of the double mutants die before embryonic day (E)12.5 (Ikeya et al., 1997).

In this study, we found that expression of Wnt1 and Wnt3a is maintained in stretched roof-plate cells. Analyses of mouse embryos with a specific defect in Wnt secretion in roof-plate cells provided evidence that supported our hypothesis that Wnt secretion by roof-plate cells is required for the proper activation of Wnt signaling in, as well as the proper proliferation of, the neural stem/progenitor cells surrounding the central canal.

RESULTS

Stretched roof-plate cells maintain physical contact with the luminal surface of the central canal

To examine changes in the morphology of roof-plate cells during development of the spinal cord in mice, we first monitored expression of the *ezrin* gene, which encodes a FERM domain-containing actin-binding protein that localizes on the apical side of epithelial cells and is expressed in roof-plate cells on E10.5 (Fig. 1A; Saotome et al., 2004). With shrinking of the spinal cord lumen after E13.5, we found that ezrin-positive roof-plate cells stretched along their dorsoventral axis (Fig. 1B-D′), consistent with observations in other species (Böhme, 1988; Kondrychyn et al., 2013). Of note, the stretched cells re-oriented so that the nuclei of these cells were aligned along the midline (Fig. 1B′).

Ezrin expression was also observed along the apical surface of the lumen from the mid-gestation stage (in the area indicated by yellow dashed brackets in Fig. 1B-D) and this complex expression pattern made it difficult to precisely follow changes in the morphology of the stretched roof-plate cells. To overcome this problem, we minimally labeled stretched roof-plate cells using a *Wnt1-CreERT* allele in conjunction with the *R26R-Confetti* reporter (Fig. 1E-K; Snippert et al., 2010; Zervas et al., 2004). Pregnant mice carrying E11.5 or E13.5 embryos were treated with a low dose of 4-hydroxytamoxifen (4OH-TM) and embryos were recovered on E13.5 or E15.5, respectively (Fig. 1E). These labeling experiments demonstrated that the nucleus of each roof-plate cell (marked by open arrowheads in Fig. 1F-H) moved in the ventral direction beginning on E13.5 and that the cell process stretched along the dorsoventral axis so that it continued to face the lumen (closed arrowheads in Fig. 1D′,F-K). Most of the processes that were labeled with membrane-bound CFP maintained contact with the lumen on both E13.5 (83.3%, n=5/6) and E15.5 (100%, n=8/8) (Fig. 1F,I), which suggests that the processes had stretched to keep their tips facing the shrinking lumen. Electron microscopic (EM) observation showed that the tips of the stretched cells were in contact with the lumen on both E13.5 and E18.5 (Fig. 2A,C). EM observation also showed that the narrow tip of the process of each roof-plate cell was aligned side by side with that of its neighboring cells (Fig. 2A,C). Furthermore, the processes of the roof-plate cells were enriched in intermediate filaments, which could be clearly identified based on their structure (Fig. 2E,G). In the area close to the lumen, a basal body structure was specifically observed, which suggested the formation of cilia (Fig. S1J). In addition, numerous vesicles were seen at the tip of the processes, suggesting active secretion of proteins via secretory vesicles (Fig. S1J). In contrast, ezrin-immunostaining of roof-plate cells also showed that the dorsal tip of the cell process extended to the spinal cord pia after E15.5 (braces in Fig. 1C,D). These results indicate that each roof-plate cell stretched along its dorsoventral axis to maintain physical contact with both the pia and shrinking lumen.

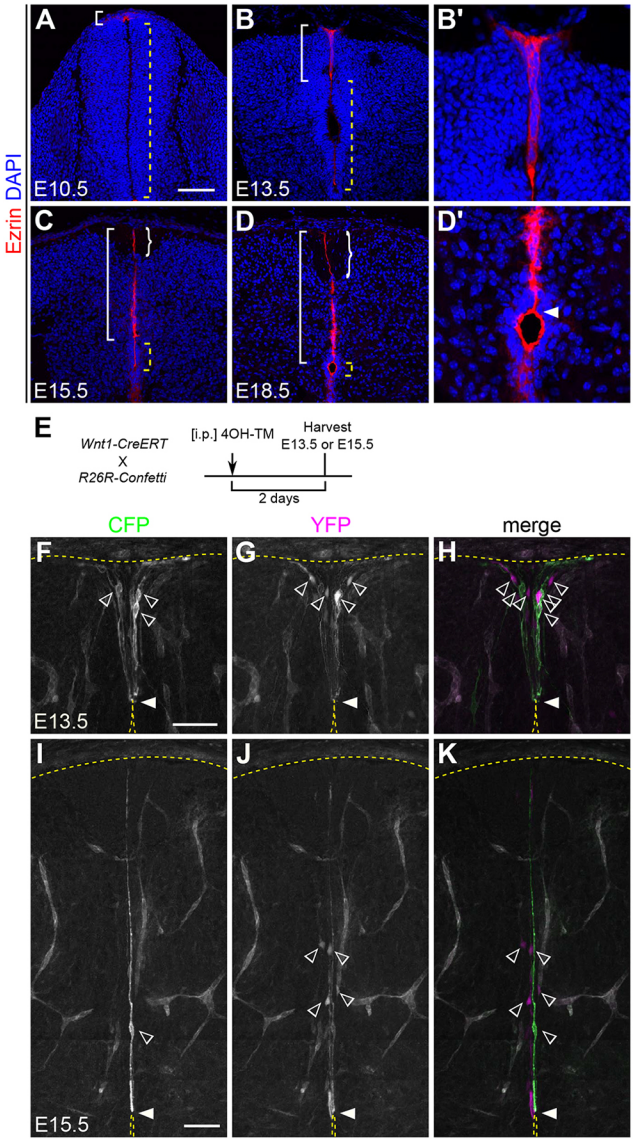

Fig. 1. Stretching of roof-plate cells in mouse embryos. (A-D′) Changes in the morphology of roof-plate cells were examined by immunohistochemistry using anti-ezrin antibody. Transverse sections at the forelimb level on E10.5 (A), E13.5 (B), E15.5 (C) and E18.5 (D) are shown. B′ and D′ show enlarged images of B and D, respectively. Nuclei were counterstained with DAPI. White brackets indicate roof-plate cells; yellow dashed brackets indicate the lumen of the spinal cord; braces (C,D) indicate processes of roof-plate cells in the white matter region of the dorsal spinal cord. Closed arrowhead indicates the ventral tip of stretched roof-plate cells. Three embryos were examined at each stage. (E-K) Examination of morphological changes in roof-plate cells at single cell resolution. Schematic of roof-plate cell labeling is shown in E. Sparsely labeled roof-plate cells were examined in E13.5 (F-H) and E15.5 (I-K) embryos harboring *Wnt1-CreERT* and *R26R-Confetti*. Transverse sections of labeled embryos at the forelimb level are shown. Pregnant mice carrying these embryos were administered low-dose 4OH-TM 2 days before observation. CFP (F,I) and YFP (G,J) indicate the plasma membrane and cytoplasm of individual cells, respectively. Merged images are also shown (H,K). Closed and open arrowheads indicate the ventral tips and nuclei of stretched roof-plate cells, respectively. Yellow dashed lines indicate the edge of the lumen and the margin of the spinal cord. Four embryos were examined. Scale bars: 100 µm in A; 50 µm in F,I.

Previous research has shown that the cell processes that are stretched along the midline in the dorsal spinal cord express nestin (Ševc et al., 2009). To examine the extent of the contribution of

Development (2019) 146, dev159343. doi:10.1242/dev.159343

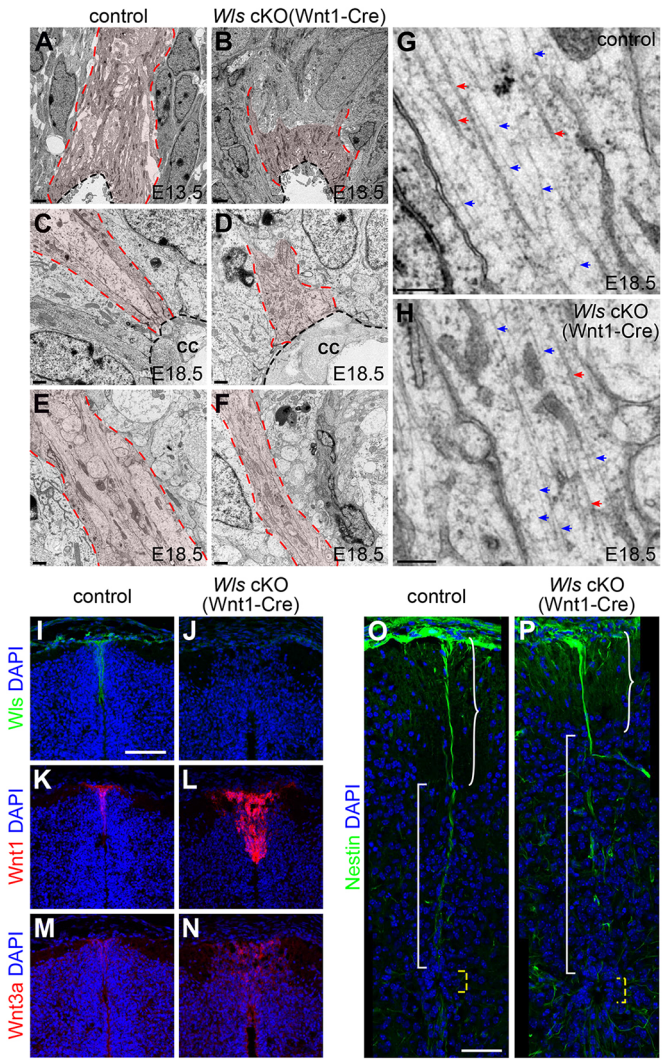

Fig. 2. Wnt secretion by roof-plate cells is required for normal morphogenesis. (A-H) Transverse section electron microscopic images at the forelimb level of stretched roof-plate cells in *Wnt1-Cre; Wls* cKO embryos (B,D,F,H) and littermate controls (A,C,E,G) on E13.5 (A,B) and E18.5 (C-H). Stretched roof-plate cells are marked in light red surrounded with red dashed lines. Black dashed lines indicate the edge of the lumen of the spinal cord, or the central canal (cc). Intermediate filaments and microtubules are indicated by blue and red arrows, respectively, in G and H. Two embryos were observed at each stage. (I-N) Impaired secretion of Wnt proteins from roof-plate cells in *Wnt1-Cre; Wls* cKO embryos. Immunohistochemistry was performed using *Wnt1-Cre; Wls* cKO embryos (J,L,N) and littermate controls (I,K,M) at the forelimb level on E13.5 with anti-Wls (I,J), anti-Wnt1 (K,L) and anti-Wnt3a (M,N) antibodies. Three embryos were examined in each experiment. (O,P) Nestin immunostaining revealed impaired morphogenesis of stretched roof-plate cells in *Wnt1-Cre; Wls* cKO embryos. Nestin staining was specifically perturbed in the gray matter area (white brackets) in *Wnt1-Cre; Wls* cKO embryos (P) compared with that in littermate controls (O). Yellow dashed brackets indicate the lumen of the spinal cord; braces indicate processes of roof-plate cells in the white matter region of the dorsal spinal cord. Three embryos were examined in each experiment. Scale bars: 2 µm in A,B; 1 µm in C-F; 0.2 µm in G,H; 100 µm in I; 50 µm in O.

progeny roof-plate cells to the formation of midline processes, we followed roof-plate progeny among nestin-positive midline cells. In this experiment, roof-plate progeny cells were labeled using a *Wnt1-CreERT* allele in conjunction with the *R26R-tdTomato* reporter (Madisen et al., 2009; Zervas et al., 2004). Pregnant mice carrying E13.5 embryos were injected with a dose of 4OH-TM for sufficient CreERT induction (2 mg of 4OH-TM per pregnant mouse), and the embryos were recovered on E18.5 (Fig. S1A-C). As shown in Fig. S1C, most of the roof-plate progeny cells labeled on E13.5 were localized along the midline of the dorsal spinal cord by E18.5. Co-staining of these tdTomato-positive cells with anti-nestin antibody revealed that the roof-plate progeny cells constituted 92.5% of the nestin-positive midline cells (197 of 213 nestin-positive cells; Fig. S1D-F). Given that the efficiency of tamoxifen-induced Cre activation is <100%, this result indicates that almost all of the nestin-positive midline cells were derived from roof-plate cells.

Similar to stretched roof-plate cells, neural progenitor cells also have a characteristic long process. The nuclei of neural progenitor cells demonstrate cell cycle-dependent movement known as interkinetic nuclear migration, during which mitosis occurs on the apical side. To determine whether elongated roof-plate cells also exhibit characteristics similar to those of neural progenitor cells, we examined the position of mitotic roof-plate cells by monitoring the phosphorylation of histone H3 (pHH3) on E12.5 and E13.5 (Fig. S1G-I). Although most of the pHH3-positive cells were detected on the apical side along the spinal cord lumen, except at the roof plate, which is marked by ezrin expression, pHH3 signals were not localized on the apical side of roof-plate cells on E12.5 (Fig. S1G,I). Furthermore, a pHH3 signal was hardly detected at the roof plate on E13.5, although the pHH3-positive cells along the spinal cord lumen were still detected (Fig. S1H,I). Therefore, the elongation of roof-plate cells did not appear to be a process that is common to all neuroepithelial cells.

Wnt expression during the stretching of roof-plate cells

To determine whether *Wnt1* and *Wnt3a* expression is maintained throughout embryogenesis in stretched roof-plate cells, we performed *in situ* hybridization experiments (Fig. S2A-D). However, only faint staining of *Wnt1* and *Wnt3a* mRNA was detected in stretched roof-plate cells (Fig. S2C,D). We therefore sought to evaluate Wnt1 and Wnt3a expression through direct detection of the endogenous distribution of Wnt1 and Wnt3a proteins; we used immunostaining with specific antibodies and also generated a line of knock-in mice in which endogenous *Wnt3a* was replaced with *egfp-Wnt3a*, which encodes Wnt3a fused in-frame with EGFP at the N-terminus [$Wnt3a^{tm(gfp\text{-}Wnt3a)}$; Fig. S3A,B]. In knock-in embryos, *egfp-Wnt3a* recapitulated the expression of endogenous *Wnt3a*, as evidenced by similarity between the GFP expression pattern and that of Wnt3a protein (Fig. S3F-H,I-L). Furthermore, in immunohistochemistry experiments using an anti-GFP antibody, we detected GFP-Wnt3a with higher sensitivity than in experiments using an anti-Wnt3a antibody. Additional confirmation that *egfp-Wnt3a* recapitulated the activity of endogenous *Wnt3a* was obtained by the absence of any change in *Axin2* expression in homozygotes, as *Axin2* is a well-known target of Wnt/β-catenin signaling (Fig. S3M,N). In addition, no obvious abnormalities were observed, which would have been expected if Wnt3a activity had been compromised (Fig. S3C-E,O; Takada et al., 1994).

In the immunostaining of wild-type embryos with anti-Wnt1 and anti-Wnt3a antibodies and of knock-in embryos with anti-GFP antibody, specific signals were observed in the dorsal-most region of the spinal cord on E10.5, as was previously shown by *in situ* hybridization (Fig. 3A; Fig. S2E-I; Fig. S3I-L; Parr et al., 1993). Signals were also detected along the apicobasal axis of roof-plate cells from E13.5 to E18.5, although there was some decrease in signal intensity on E18.5 (Fig. 3B-D). Thus, embryonic *Wnt1* and

Development (2019) 146, dev159343. doi:10.1242/dev.159343

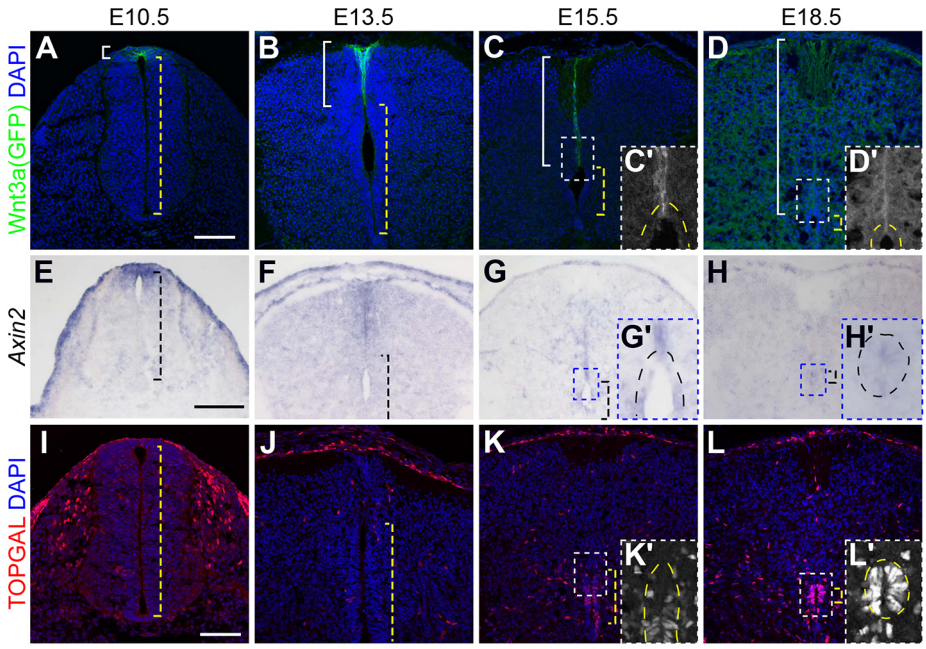

Fig. 3. Wnt ligand and signaling in the developing mouse spinal cord. (A-D′) Distribution of Wnt3a proteins at the forelimb level in the developing spinal cord on E10.5 (A), E13.5 (B), E15.5 (C) and E18.5 (D). Insets C′ and D′ show enlarged images of the white dashed outlines in C and D, respectively. Transverse sections of *Wnt3a*$^{tm(GFP\text{-}Wnt3a)}$ homozygous embryos were stained with anti-GFP antibody. Nuclei were counterstained with DAPI. Roof-plate cells are indicated by white brackets; yellow dashed brackets indicate the lumen of the spinal cord; yellow dashed lines (C′ and D′) indicate the outer edges of the cells around the central canal. Three embryos were examined at each stage. (E-H′) Wnt/β-catenin signaling was visualized by monitoring the expression of *Axin2* in the developing spinal cord at the forelimb level on E10.5 (E), E13.5 (F), E15.5 (G) and E18.5 (H). Insets G′ and H′ show enlarged images of the blue dashed outlines in G and H, respectively. Dashed brackets indicate the lumen of the spinal cord; dashed lines (G′ and H′) indicate the outer edges of the cells around the central canal. Three embryos were examined at each stage. (I-L′) Wnt/β-catenin signaling was visualized using a transgenic embryo harboring the TOPGAL reporter in the developing spinal cord at the forelimb level on E10.5 (I), E13.5 (J), E15.5 (K) and E18.5 (L). Insets K′ and L′ show enlarged images of the white dashed outlines in K and L, respectively. TOPGAL signals were examined by immunohistochemistry using anti-β-galactosidase antibody. Nuclei were counterstained with DAPI. Three embryos were examined at each stage. Yellow dashed brackets indicate the lumen of the spinal cord; yellow dashed lines indicate the outer edges of cells around the central canal. Scale bars: 100 µm.

Wnt3a expression continues during and shortly after the morphological change in roof-plate cells. In addition to these midline signals, Wnt1, Wnt3a and GFP-Wnt3a proteins were detected in the margin of the dorsal spinal cord on E10.5 and E13.5. Importantly, GFP-Wnt3a was detected up to the tip of the process of stretched roof-plate cells (Fig. 3C-D′), which indicates that endogenous Wnt was delivered to the tip of the process that faces the lumen of the central canal.

We next assessed Wnt signaling activity by monitoring *Axin2* expression, which is activated by Wnt/β-catenin signaling (Fig. 3E-H′; Jho et al., 2002), or using a transgenic embryo harboring the ins-TOPGAL (TOPGAL) reporter gene (Fig. 3I-L′; Moriyama et al., 2007). Before roof-plate cell stretching, *Axin2* is expressed in the dorsal spinal cord (Fig. 3E; Jho et al., 2002), consistent with the distribution of Wnt1 and Wnt3a (Fig. 3A; Fig. S2E,H). From E13.5 to E15.5, *Axin2* expression was evident in stretched roof-plate cells (Fig. 3F,G), whereas its expression was reduced on E18.5 (Fig. 3H). In addition, a web-like pattern of weak *Axin2* expression was observed in the middle of a transverse section of the spinal cord (Fig. 3G,H), which most likely corresponded to the previously reported activation of Wnt/β-catenin signaling in developing vessels (Stenman et al., 2008). On the other hand, as has been previously shown by a number of TOPGAL reporter analyses, Wnt signaling in the roof-plate cells was hardly detectable by this method; although this signaling in neural crest cells was detectable on E10.5 (Fig. 3I). From E15.5 to E18.5, TOPGAL expression was also detected in ependymal cells that surround the central canal, towards which the tips of the stretched roof-plate cells faced (Fig. 3K-L′). Therefore, consistent with the expression of *Wnt1* and *Wnt3a* in stretched roof-plate cells, Wnt/β-catenin signaling that was detectable by *Axin2* expression was activated in these cells. In addition, Wnt/β-catenin signaling that was detected by the TOPGAL reporter was also activated in cells in close proximity to the tip of the roof-plate cell processes.

Wnt secretion by roof-plate cells is required for coordinated rearrangement of cells during stretching

Next, we examined the role of Wnt expressed in the roof-plate cells by inhibiting its secretion by these cells. We generated embryos with a specific conditional knockout (cKO) of *Wls*, which is required for Wnt secretion (Goodman et al., 2006; Bartscherer et al., 2006; Bänziger et al., 2006). The knockout mutant embryos were constructed using a floxed *Wls* allele and *Wnt1-Cre* transgene (Carpenter et al., 2010; Danielian et al., 1998). Although abundant expression of Wls was detected in the dorsal midline of the spinal cord of littermate controls on E13.5 (Fig. 2I), almost no immunoreactivity to Wls was detected in this region in the *Wls* cKO embryos (Fig. 2J). In contrast to littermate controls, *Wls* cKO embryos exhibited abundant expression of Wnt1 and Wnt3a proteins across an area wider than the roof plate (Fig. 2K-N). Considering that progeny cells of roof-plate cells were distributed outside the roof plate at this stage (Fig. S4), defective secretion of Wnt proteins is likely to be the reason for the prolonged persistence of Wnt1 and Wnt3a proteins within the progeny cells in *Wls* cKO embryos.

Development (2019) 146, dev159343. doi:10.1242/dev.159343

As in the case of *Wnt1* and *Wnt3a* compound mutant embryos, patterning of the dorsal neural tube was impaired in the *Wls* cKO embryos on E10.5 (Fig. S5; Muroyama et al., 2002). On E13.5, *Wls* cKO embryos exhibited a malformed head, a predictable defect that is caused by a lack of Wnt signaling in the roof plate (Fig. S6A-E). An examination of transverse sections of the spinal cord revealed a shortened dorsal (but not ventral) spinal cord (Fig. S6F-H), probably resulting from a defect in cell proliferation caused by the loss of Wnt signaling during the early stages of roof-plate formation. EM observations showed that the alignment of the tips of the stretched roof-plate cells was disturbed in the *Wls* cKO embryos (Fig. 2A-D). In addition, EM observations and immunostaining for nestin showed that the bundle of the processes of roof-plate cells appeared to be thinner and was frequently branched in the *Wls* cKO embryos (Fig. 2E,F,O,P; Fig. S6I,I′), although the cytoskeletal structures appeared to have formed properly (Fig. 2G,H). In contrast, no obvious change in the distribution of acetylated tubulin was detected in the *Wls* cKO embryos (Fig. S6J,K). These results indicate that Wnt secreted by roof-plate cells is required for the coordinated changes in roof-plate cell morphology that occur during normal development.

To further explore this morphological defect in *Wls* cKO mutant embryos, we examined the development of roof-plate cells in earlier stages of embryogenesis (Fig. 4). On E13.5, when stretching is first observed in normal embryos, roof-plate cells appeared to be elongated along the midline based on ezrin expression, forming a 'train' of cells, as described above (Fig. 4B,E,H). By contrast, in *Wls* cKO mutant embryos the ezrin-positive cells did not rearrange in a train-like manner (Fig. 4C,F,I). Thus, defective coordination of roof-plate cells on E13.5 in *Wls* cKO mutant embryos (Fig. 4J) appears to have induced the morphological abnormality that is evident in these cells in later stages. Because Wnt signaling was active in roof-plate cells during stretching, it appears to be plausible that Wnt activity was directly involved in this rearrangement. However, as the number of ezrin-positive cells was slightly increased in *Wls* cKO mutant embryos (Fig. S7), it also appears to be possible that the defective rearrangement of ezrin-positive roof-plate cells was inhibited by crowding of roof-plate cells in these embryos.

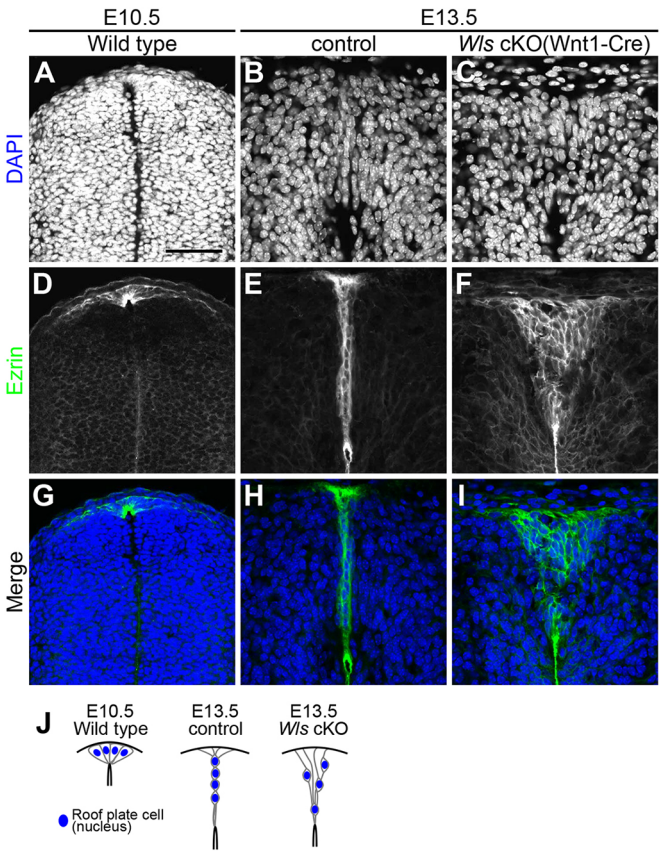

Fig. 4. Wnt secretion is required for normal rearrangement of roof-plate cells. (A-I) Transverse sections at the forelimb level showing cell rearrangement in *Wnt1-Cre; Wls* cKO embryos (C,F,I) and littermate controls (A,B,D,E,G,H) on E10.5 (A,D,G) and E13.5 (B,C,E,F,H,I) using DAPI staining (A-C) and an anti-ezrin antibody (D-F); merged images are shown in G-I. (J) Schematic of the morphology of roof-plate cells shown in A-I. Three embryos were examined in each experiment. Scale bar: 50 µm.

Cells surrounding the central canal in *Wls*-defective embryos exhibit impaired Wnt signaling

As described in the section 'Wnt expression during the stretching of roof-plate cells', expression of the TOPGAL reporter was detected in ependymal cells on E18.5 (Fig. 3L′). As the ventral tip of the stretched roof-plate cells faced the dorsal surface of the central canal, we hypothesized that Wnt proteins secreted by roof-plate cells were required for this Wnt/β-catenin signaling detected by the TOPGAL reporter. To support this idea, we observed the delivery of GFP-Wnt3a proteins up to the tip (Fig. 3C′,D′), and numerous vesicles at the tip, which suggested active secretion of proteins via secretory vesicles (Fig. S1J). We further tested this hypothesis from several different aspects.

As *Wls* is essential for the secretion of Wnt proteins, we examined the expression of TOPGAL reporter in ependymal cells in *Wls* cKO embryos. In contrast to littermate controls, *Wls* cKO embryos exhibited a significant reduction in the frequency of TOPGAL-positive cells among ependymal cells on E15.5 and E18.5 (Fig. 5A-F). Furthermore, this reduction was more severe in the ependymal cells that lined the dorsal half of the central canal (Fig. 5D-F). It therefore appears to be plausible that Wnt proteins secreted by roof-plate cells are specifically required for activation of Wnt/β-catenin signaling in some of the dorsal ependymal cells. On the other hand, our findings also suggested that some other Wnt proteins that had not been secreted by roof-plate cells activated Wnt/β-catenin signaling in other ependymal cells.

However, as it still appeared to be possible that the defects in Wnt signaling in dorsal ependymal cells in *Wls*-cKO embryos could have been a secondary consequence of impaired *Wls* function in earlier developmental stages, we next tried to suppress the function of *Wls* after the onset of roof-plate stretching by using a floxed *Wls* allele and *Wnt1-CreERT* transgene (Carpenter et al., 2010; Zervas et al., 2004). To distinguish *Wls* cKO embryos generated using *Wnt1-CreERT* from those generated by *Wnt1-Cre*, henceforward, we refer to the former as *Wnt1-CreERT; Wls* cKO and the latter as *Wnt1-Cre; Wls* cKO embryos. Pregnant mice were injected with 4OH-TM every other day from day 13.5 post coitum (Fig. 6A-C). The resulting *Wnt1-CreERT; Wls* cKO embryos exhibited no obvious abnormalities in terms of the morphology of stretched roof-plate cells, as assessed by immunohistochemistry using an anti-nestin antibody and by EM observations (Fig. 6D-G; Fig. S8A-C). In contrast, Wnt signaling was specifically reduced in the ependymal cells in these embryos (Fig. 6H-J; Fig. S8D-G). This result indicates that the reduced Wnt activation that was observed in ependymal cells in *Wnt1-Cre; Wls* cKO embryos, as described above, was not a secondary result of the morphological

Development (2019) 146, dev159343. doi:10.1242/dev.159343

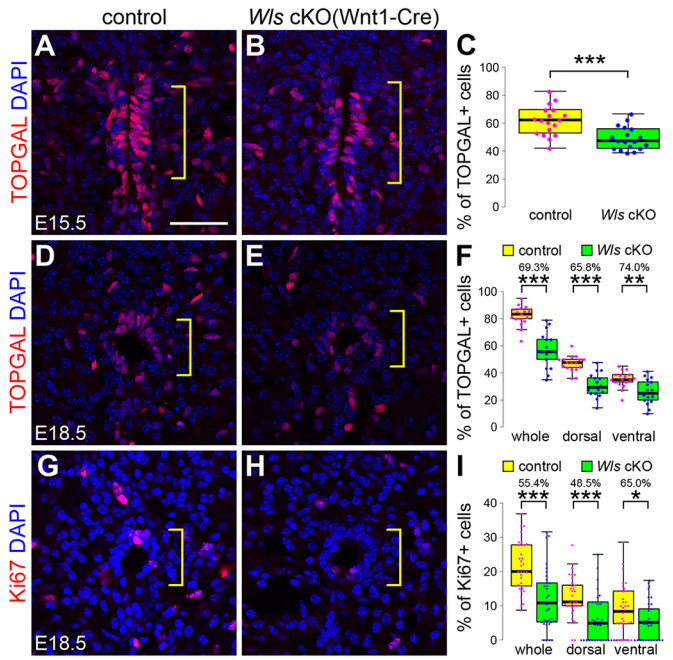

Fig. 5. Wnt signaling activity and proliferation of cells surrounding the central canal in *Wls* cKO mice during development. (A-I) Wnt signaling activity (A-F) and proliferation (G-I) of the cells surrounding the central canal in *Wnt1-Cre; Wls* cKO embryos on E15.5 (A-C) and E18.5 (D-I) were examined in transverse sections at the forelimb level. Wnt signaling was examined using the TOPGAL reporter in *Wnt1-Cre; Wls* cKO embryos (B,E) and in littermate controls (A,D). Expression of TOPGAL reporter was examined using anti-β-galactosidase antibody. A statistical summary of this experiment is shown in C and F. Cell proliferation was assessed by monitoring the expression of Ki67 (red) using immunohistochemistry in *Wnt1-Cre; Wls* cKO embryos (H) and in littermate controls (G). A statistical summary of this experiment is shown in I. Nuclei were counterstained with DAPI. Brackets indicate ependymal cells lining the central canal. **P*<0.05, ***P*<0.01, ****P*<0.001 (Student's *t*-test). In F and I, the percentage of positive cells in embryos of *Wnt1-Cre; Wls* cKO and control mice is indicated. Three embryos each were examined in A,B,D,E and six embryos each were examined in G and H. A total of 18, 17 and 34 sections were analyzed in C,F and I, respectively. Box plots indicate the first and third quartiles and the median. Scale bar: 50 µm.

defect in the stretched roof-plate cells or any other defect that occurred before E13.5.

On the other hand, it also remained possible that roof-plate progenies had differentiated into ependymal cells during or after the stretching and that Wnt signaling remained activated in these cells. To examine the contribution of progeny roof-plate cells to the formation of ependymal cells, we labeled roof-plate progenies using a *Wnt1-CreERT* allele in conjunction with the *R26R-tdTomato* reporter (Fig. 6N-P). On E18.5, we hardly detected roof-plate progenies among the ependymal cells; only in a few sections did we observe roof-plate progenies in the most dorsal portion of the area surrounding the central canal, and the average number of these progenies in this area was slightly increased on postnatal day 4 (Fig. 6O,P; Fig. S9). As the number of roof-plate progenies among the ependymal cells was significantly low compared with that of the roof plate-dependent increase in the number of Wnt-active cells (Fig. 6P; Fig. S8G,H), the results obtained from these two types of *Wls*-cKO embryos strongly suggest that Wnt secretion by stretched roof-plate cells is required for activation of Wnt signaling in the ependymal cells that surround the dorsal central canal on E18.5. As most ependymal cells are derived from the p2 and pMN domains in the ventral spinal cord, in which Wnt/β-catenin signaling is not activated before stretching, rather than from roof-plate cells (Fig. 6O; Fig. S1C; Yu et al., 2013), our results appear to indicate that stretching of the roof-plate cells altered the target cells of the Wnt signals that are secreted by roof-plate cells.

Cells surrounding the central canal in *Wls*-defective embryos exhibit impaired cell proliferation

Neural stem cells have been identified in the ependymal zone that surrounds the central canal in the adult spinal cord (Johansson et al., 1999; Martens et al., 2002; Weiss et al., 1996). Therefore, we next investigated whether Wnt proteins secreted by roof-plate cells could be required for the proliferation of ependymal cells. On E18.5, *Wnt1-Cre; Wls* cKO mutant embryos exhibited a significant decrease in the frequency of Ki67 (also known as Mki67)-immunoreactive proliferating cells among the ependymal cells (Fig. 5G-I). Furthermore, ependymal cells surrounding the dorsal half of the central canal exhibited more severe defects on E18.5 than the cells surrounding the ventral half (Fig. 5I). A similar decrease in the frequency of Ki67-immunoreactive proliferating cells was observed in *Wnt1-CreERT; Wls* cKO embryos recovered from pregnant mice that had been injected with 4OH-TM every other day from day 13.5 post coitum (Fig. 6K-M). Furthermore, compared with the contribution of roof-plate progenies to the formation of ependymal cells (Fig. 6N-P), the effect of Wls-deficiency on proliferation of ependymal cells was evident. Based on these results, we concluded that Wnt secretion by stretched roof-plate cells was required for normal proliferation of the ependymal cells surrounding the central canal, at least on E18.5.

Proliferation of ependymal cells after spinal cord injury is impaired in *Wls* cKO mice

In normal adult mice, neurogenesis rarely occurs in the spinal cord; rather, after injury to the spinal cord, ependymal cells generate progeny that undergo multiple fates, which suggests that ependymal cells exhibit latent neural stem cell properties (Johansson et al., 1999; Meletis et al., 2008; Shechter et al., 2007; Habib et al., 2016). We therefore examined whether Wnt secretion by roof-plate cells is required to induce the proliferation of ependymal cells after spinal cord injury in adult mice. As *Wnt1-Cre; Wls* cKO mice die immediately after birth, we compared the effect of spinal cord injury between control and *Wnt1-CreERT; Wls* cKO mice from a mother that had been injected with 4OH-TM every other day from E12.5 to E16.5 (Fig. 7A). In control embryos, proliferation of ependymal cells, as assessed by the presence of cells that are positive for both Ki67 and vimentin, was generally activated 2 days after spinal cord injury (Fig. 7B; Fig. S10A-D). In contrast, injury-induced proliferation of ependymal cells was suppressed in the *Wnt1-CreERT; Wls* cKO mice (Fig. 7C,D). Furthermore, cells in the dorsal half of the central canal exhibited a more severe defect than the cells in the ventral half (Fig. 7D). These data demonstrate that Wnt secretion by roof-plate cells is required for the normal proliferation of dorsal ependymal cells after injury to the spinal cord. In contrast, proliferation of ventral ependymal cells was not decreased after spinal cord injury, suggesting that Wnt ligands were reactivated in the ventral spinal cord independently of roof-plate cells.

Interestingly, expression of Wnt1 (but not Wnt3a) was reactivated on the injured side of the spinal cord and along the stretched roof-plate cells extending between the pia and central canal 2 days after spinal cord injury (Fig. 7E-G; Fig. S10E,F). Furthermore, Wls expression was also reactivated in the stretched roof-plate cells (Fig. S10G-H′), which suggests that Wnt1 secretion was reactivated in stretched roof-plate cells after spinal cord injury. In contrast, apparent reduction of Wnt1 reactivation was observed in stretched

Development (2019) 146, dev159343. doi:10.1242/dev.159343

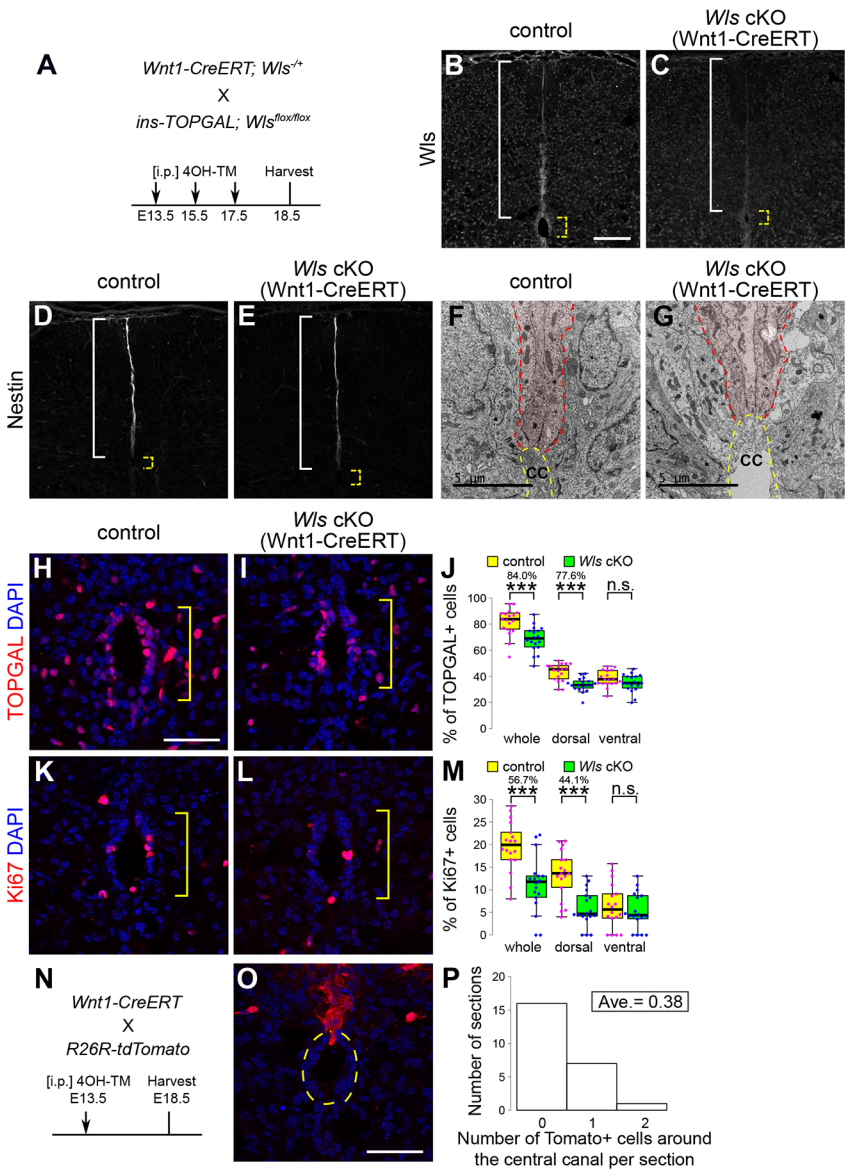

Fig. 6. Late gestation stage-specific impairment of Wnt secretion by roof-plate cells. (A) Schematic depicting reduced Wnt secretion by roof-plate cells. (B-M) Transverse sections at the forelimb showing phenotype of embryos defective in Wnt secretion by roof-plate cells specifically during late-gestation stages. *Wnt1-CreERT; Wls*$^{-/floxed}$ embryos (C,E,G,I,L) treated with 4OH-TM on E13.5, E15.5 and E17.5 (referred to hereafter as *Wnt1-CreERT; Wls* cKO embryos) were analyzed in comparison with littermate controls (B,D,F,H,K) on E18.5. Immunohistochemistry using an anti-Wls (B,C) antibody showed reduced expression of Wls in *Wnt1-CreERT; Wls* cKO embryos. Immunohistochemistry with anti-nestin (D,E) and EM observations (F,G) revealed no obvious abnormalities in the morphology of stretched roof-plate cells in *Wnt1-CreERT; Wls* cKO embryos. Wnt signaling activity (H-J) and proliferation (K-M) of cells surrounding the central canal (cc) were also examined as shown in Fig. 5. Statistical summaries of Wnt signaling and cell proliferation are shown in J and M, respectively, which indicate the percentage of positive cells in embryos of *Wnt1-Cre; Wls* cKO and control mice. These results show that Wnt signaling activity and proliferation of cells surrounding the central canal were impaired in *Wnt1-CreERT; Wls* cKO embryos. In B-E, white brackets indicate roof-plate cells and yellow dashed brackets indicate the lumen of the spinal cord. In F and G, light red area surrounded with red dashed lines indicates stretched roof-plate cells and yellow dashed lines indicate the edge of the lumen of the spinal cord. In H,I,K,L, yellow brackets indicate ependymal cells lining the central canal. Three embryos were examined for immunohistochemistry, two embryos were examined for EM analyses and 18 sections were analyzed for the statistical analyses. ***P<0.001 (Student's t-test). n.s., not significant. Box plots indicate the first and third quartiles and the median. (N-P) Distribution of the progeny of roof-plate cells labeled on E13.5. Schematic shows lineage tracing of roof-plate cells using E18.5 embryos carrying *Wnt1-CreERT* and *R26R-tdTomato* (N). Transverse sections at the forelimb level were stained with anti-RFP antibody (O); yellow dashed line indicates the outer edge of ependymal cells. A statistical summary indicating the average number of tomato-positive cells per section is shown in P. Twenty-four sections prepared from five embryos were examined. Nuclei were counterstained with DAPI (H,I,K,L, O). Scale bars: 100 μm in B; 5 μm in F,G; 50 μm in H,O.

roof-plate cells of *Wnt1-CreERT; Wls* cKO mice, although reactivation in other areas of the spinal cord was only slightly affected by spinal cord injury (Fig. 7F-J). Therefore, reactivation of Wnt1 secretion by roof-plate cells appears to play a role in promoting ependymal cell proliferation and Wnt signaling.

DISCUSSION

The roof plate functions as an organizing center during the development of the dorsal spinal cord. Considerable evidence has shown that Wnt produced by roof-plate cells plays multiple roles before the stretching of the roof plate (Ikeya et al., 1997;

Development (2019) 146, dev159343. doi:10.1242/dev.159343

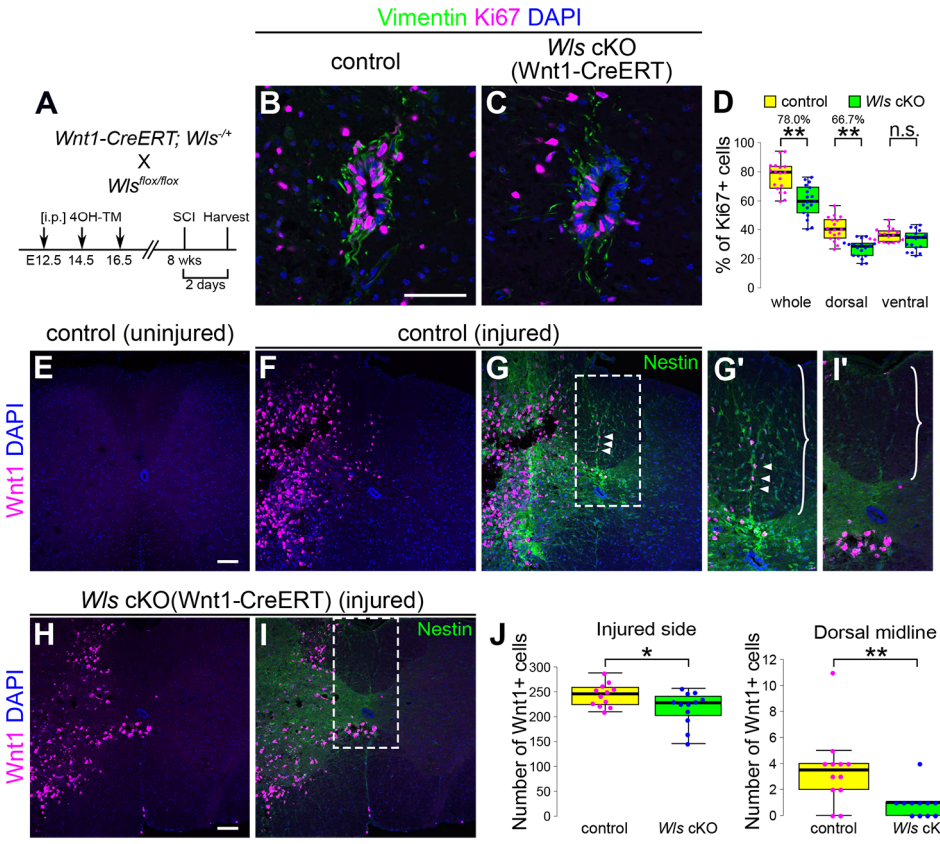

Fig. 7. Proliferation of cells surrounding the central canal in *Wls* cKO mice after spinal cord injury. (A) Procedure of the experiments. (B-D) Proliferation of cells surrounding the central canal during regeneration after spinal cord injury in embryos of *Wnt1-CreERT; Wls* cKO mice 8 weeks after birth. *Wnt1-CreERT; Wls*$^{-/floxed}$ mice treated with 4OH-TM on E12.5, E14.5 and E16.5 (referred to hereafter as *Wnt1-CreERT; Wls* cKO mice) were analyzed in comparison with littermate controls. Cell proliferation was assessed by monitoring the expression of Ki67 in transverse sections of *Wnt1-CreERT; Wls* cKO mice (C) and littermate controls (B) at the forelimb level. Sections with DAPI and anti-vimentin antibody to visualize nuclei and ependymal cells, respectively. A statistical summary indicating the percentage of positive cells in mice of *Wnt1-CreERT; Wls* cKO and control mice is shown in D. ***P*<0.01 (Student's *t*-test). n.s., not significant. Six mice were examined for each mouse type and 18 sections were used for the statistical analyses. (E-J) Wnt1 expression at the forelimb level in uninjured wild-type mice at 8 weeks after birth (E) and 8-week-old wild-type (F,G) and *Wnt1-CreERT; Wls* cKO (H,I) mice 2 days after spinal cord injury. The left was the injured side (F-I). To visualize the midline of the spinal cord, we stained sections with anti-nestin antibody (green; G,I). G′ and I′ show enlarged images of the boxed sections in G and I, respectively. Nuclei were counterstained with DAPI. Braces (G′,I′) indicate the white matter region of the dorsal spinal cord; arrowheads indicate Wnt1-positive cells in the midline of the spinal cord. Statistical summaries indicating the number of Wnt1-positive cells are shown in J. **P*<0.05, ***P*<0.01 (Student's *t*-test). Three mice were examined for each mouse type and 12 sections examined for statistical analyses. Box plots indicate the first and third quartiles and the median. Scale bars: 50 µm in B; 100 µm in E,H.

Ikeya and Takada, 1998; Muroyama et al., 2002; Riccomagno et al., 2005). For example, Wnt1 and Wnt3a expressed by roof-plate cells play roles in regulating the proliferation and specification of neural progenitor cells in the dorsal neural tube (Lee et al., 2000; Muroyama et al., 2002). After stretching, the apical tips of the processes of roof-plate cells become close to the ependymal cells that surround the central canal. Notably, our experiments using GFP-Wnt3a knock-in embryos showed that endogenous Wnt proteins are delivered to the tip of the elongated processes. Use of the TOPGAL reporter showed that Wnt signaling is activated in the ependymal cells that surround the central canal, but that this signaling is impaired in *Wnt1-CreERT; Wls* cKO embryos, in which *Wls* expression is impaired almost exclusively in elongated roof-plate cell progeny after E13.5. Therefore, Wnt proteins secreted from the roof-plate cells appear to have another role, in addition to their earlier roles in the organizing center. Considering that most ependymal cells originate from cells in the ventral region, p2 and pMN domains (Yu et al., 2013) of the spinal cord, our results strongly suggest that the stretching morphogenesis of signal-producing cells results in a change in the signal-receiving cells during the development of the spinal cord.

Interestingly, our data also indicate that Wnt proteins play a role in the morphogenesis of signal-producing cells. In *Wnt1-Cre; Wls* cKO embryos, the development of roof-plate cells, which produce Wnt1 and Wnt3a, is impaired. That is, coordinated rearrangement of the stretched roof-plate cells does not occur on E13.5, and this defect likely causes morphological abnormalities in these cells during later stages of development. These findings suggest that Wnt proteins actively regulate the change in cell morphology, thus revealing a novel function. Similarly, signaling by other molecules is required for the formation and maintenance of cell processes that are involved in the intercellular transfer of signaling proteins (Hsiung et al., 2005; Roy et al., 2014; Inaba et al., 2015). However, we cannot exclude another possible explanation for the abnormal morphology of roof-plate cells in *Wnt1-Cre; Wls* cKO embryos. The reduced proliferation of dorsal spinal cord cells in response to the reduction in Wnt secretion by roof-plate cells before their stretching could, in turn, affect the stretched morphogenesis of the roof-plate cells. In addition, as roof-plate cell progeny are distributed across a

Development (2019) 146, dev159343. doi:10.1242/dev.159343

wide area of the spinal cord, we must consider the distribution of these cells in *Wnt1-Cre; Wls* cKO embryos. More-extensive analyses could perhaps clarify the mechanism by which roof-plate cells stretch during normal development of the spinal cord.

It is thought that intercellular signals regulate neural progenitors in both embryos and adults. For instance, Wnt signaling regulates the population of neural stem/progenitor cells in the subventricular zone (SVZ) of the cerebrum and the subgranular zone of the hippocampus in adult mammals (Adachi et al., 2007; Bowman et al., 2013; Lie et al., 2005; Maretto et al., 2003). Brain injury leads to an increase in Wnt signaling in the SVZ (Piccin and Morshead, 2011). However, despite the importance of these intercellular signals, which cells provide signaling proteins to the neural cell precursors remains a matter of debate. In the spinal cord, neural stem/progenitor cells are among the population of ependymal cells that surround the central canal, which is connected to the brain ventricle (Johansson et al., 1999; Meletis et al., 2008; Weiss et al., 1996). In this study, we showed that the proliferation of ependymal cells, including neural stem/progenitor cells, is also regulated by intercellular signals. The proliferation of ependymal cells is promoted via the close proximity of roof-plate cells resulting from their stretching. As Wnt signaling by ependymal cells is enhanced as a result of roof-plate cell stretching, it is plausible to conclude that Wnt is a ligand that is secreted by stretched roof-plate cells to activate neural progenitor/stem cells in the spinal cord. An interesting area of future study is whether brain neural progenitors are also regulated by the long-range transport of Wnt proteins that is mediated by stretched roof-plate cells, as in the case of the spinal cord.

Finally, we recognize that Xing et al. (2018) also reported that roof-plate cells are responsive to Wnt signaling by utilizing *Axin2-CreERT2* mice during the revision period of this paper. They showed that the Wnt-responsive cells contribute to the ependymal cells of the spinal cord in the adult mouse. In contrast, our study identified Wnt ligands that are expressed in stretched roof-plate cells and showed evidence that secretion of these Wnt ligands increased Wnt signaling in ependymal cells and was specifically required for proliferation. Furthermore, we also showed the requirement for Wnt in roof-plate cells for response to spinal cord injury. Thus, Wnt signals appear to regulate ependymal cells in several distinct ways.

MATERIALS AND METHODS

Mice

This study was performed in accordance with the Guidelines for Animal Experimentation of the National Institutes of Natural Sciences, with approval of the Institutional Animal Care and Use Committee of the National Institutes of Natural Sciences (#15A183, #16A071, #17A062). Every effort was made to minimize animal suffering during experimental procedures.

EIIa-Cre (Lakso et al., 1996), *ins-TOPGAL* (Moriyama et al., 2007), *R26R-Confetti* (Snippert et al., 2010), *R26R-tdTomato* (Madisen et al., 2009), *Wls flox* (Carpenter et al., 2010), *Wnt1* KO (McMahon and Bradley, 1990), *Wnt1-Cre* (Danielian et al., 1998), *Wnt1-CreERT* (Zervas et al., 2004) and *Wnt3a* KO (Takada et al., 1994) mice have been previously described. To generate *egfp-Wnt3a* knock-in mice, FLAG-EGFP was integrated into exon 1 of the gene encoding Wnt3a, immediately behind the signal peptide, and the gene was inserted into the DT-A-pA/loxP/PGK-Neo-pA/loxP vector (www.cdb.riken.go.jp/arg/cassette.html). The neomycin cassette was removed by crossing with *EIIa-Cre* mice. Genotyping was carried out by PCR using the following primers: Wnt3a-E1F, 5′-ATGGC-TCCTCTCGGATACCT-3′; Wnt3a-I1R, 5′-ACTTTCACTGCCCTCCCT-TC-3′; and GFP-R1, 5′-TCACGAACTCCAGCAGGACCATG-3′. The wild-type, homozygous and heterozygous genotypes were indicated by a 290-bp fragment, a 756-bp fragment and both fragments, respectively.

Tissue processing

Before E13.5, embryos were fixed in 3.5% paraformaldehyde (PFA) for 30 min or overnight at 4°C. Embryos older than E15.5 were perfused with 4% PFA via the heart. Eight-week-old mice were overdosed with sodium pentobarbital (70 mg/kg) and perfused via the heart with PBS followed by 4% PFA. The spinal cord was dissected and post-fixed overnight at 4°C.

Immunohistochemistry

Immunohistochemistry was performed on cryosections of tissue as described below. Sections were incubated overnight at 4°C with the following primary antibodies : anti-β-galactosidase (PM049, MBL International; 1:400), anti-ezrin (ab4069, Abcam; 1:400), anti-GFP (598, MBL International; 1:500), anti-Gpr177 (ab176376, Abcam; 1:400), anti-Ki67 (ab16667, Abcam; 1:1000), anti-mash1 (556604, BD Pharmingen; 1:400), anti-nestin (60051A, BD Pharmingen; 1:500), anti-phospho-histone H3(Ser10) (06-570, Upstate; 1:400), anti-RFP (PM005, MBL International; 1:500), anti-tubulin, acetylated (T6793, Sigma-Aldrich; 1:1000), anti-vimentin (V2258, Sigma-Aldrich; 1:500), anti-Wnt1 (ab15251, Abcam; 1:200) and anti-Wnt3a (1:10 dilution; Takada et al., 2006). The cryosections were then incubated with secondary antibodies at a 1:500 dilution for 2 h at room temperature. In this study, the following secondary antibodies were used: goat anti-mouse IgG Alexa Fluor 488 (A-11029, Invitrogen), goat anti-mouse IgM Alexa Fluor 488 (A-21042, Invitrogen), goat anti-mouse IgG Alexa Fluor 647 (A-21235, Invitrogen) and goat anti-rabbit IgG Alexa Fluor 555 (A-21429, Invitrogen). The tissue sections were counterstained with DAPI (Dojindo). Wnt1 signals were amplified using a TSA Plus kit (PerkinElmer). To obtain Wnt3a signals, embryos were fixed in 3.5% PFA for 30 min at 4°C, and then the antigen was retrieved by incubation in Antigen Unmasking Solution (Vector Laboratories) for 15 min at 95°C. Fluorescent images were acquired using an inverted confocal microscope (Nikon A1Rsi).

In situ hybridization

Cryosections were subjected to *in situ* hybridization as follows. Briefly, sections were re-fixed with 4% PFA for 15 min at room temperature, washed with PBS, treated with 6 µg/ml of proteinase K for 20 min, incubated in 0.2 M HCl for 10 min and then acetylated using 0.1 M triethanolamine and 0.25% acetic anhydride. The sections were then incubated in hybridization buffer (50% formamide, 5× SSC, 1% SDS, 50 µg/ml tRNA and 50 µg/ml heparin) overnight at 55°C. Probes were fragmented to ∼300 bases by alkaline hydrolysis. The next day, the sections were washed with 2× SSC/50% formamide, treated with 10 µg/ml RNaseA in TNE for 30 min at 37°C, and then washed consecutively with 2× SSC, 0.2× SSC, and Tris-buffered saline with Tween 20 (TBST). The sections were incubated with 1% blocking reagent (Roche) in TBST for 1 h and then treated with a 1:500 dilution of anti-digoxigenin-AP Fab fragments (Roche) overnight at 4°C. The following day, the sections were washed with TBST and alkaline phosphatase buffer (NTMT), and signals were developed using BM Purple (Roche). The following probes were used: *Axin2* (Jho et al., 2002), *Wnt1* (Parr et al., 1993) and *Wnt3a* (Roelink and Nusse, 1991).

Labeling experiments

R26R-Confetti mice were crossed with *Wnt1-CreERT* mice. To induce Cre-mediated recombination, pregnant mice were injected with 1 mg of 4OH-TM dissolved in ethanol, dimethyl sulfoxide and sesame oil on E11.5 or E13.5. The spinal cord was harvested on E13.5 or E15.5 after perfusion fixation. Sections were cut using a vibrating microtome at a thickness of 400 µm. Images were captured using a multiphoton microscope (Leica TCS SP8 MP).

Spinal cord injury

Eight-week-old mice were anesthetized via intraperitoneal injection of a mixture of medetomidine (0.3 mg/kg), midazolam (4 mg/kg) and butorphanol (5 mg/kg). A laminectomy was performed at the level of T13. A right lateral hemisection injury was created with the tip of a scalpel. After the procedure, the mice were awakened via intraperitoneal injection of atipamezole (0.3 mg/kg). Mice were sacrificed by perfusion with PFA 1, 2 or 6 days after spinal cord injury.

Development (2019) 146, dev159343. doi:10.1242/dev.159343

Electron microscopy

Embryos were perfused via the heart with a mixture of 2% PFA, 2.5% glutaraldehyde and 100 mM sodium cacodylate buffer. The spinal cord was dissected and post-fixed for 2 h at room temperature in the same fixative.

Quantification and statistical analysis

Statistical analyses were performed using Excel and R software (version 3.5.1). Differences were assessed for statistical significance using the Student's *t*-test. A P value of <0.05 was considered indicative of statistical significance. Error bars in figures represent the standard error of the mean for each group.

Acknowledgements

We thank Drs Abe and Kiyonari for generating the GFP-Wnt3a knock-in allele, Drs Kadomatsu and Morozumi for their support in producing spinal cord injury, Ms Misaki and Takahashi for their technical support in EM observation, Drs Ikenaka, Ishino and Kitadate for their technical advice regarding experiments and the Functional Genomics Facility and Spectrography and Bioimaging Facility of the NIBB Core Research Facilities for their technical support. All members of S.T.'s laboratory are gratefully acknowledged for their helpful discussions.

Competing interests

The authors declare no competing or financial interests.

Author contributions

Conceptualization: T.S., S.T.; Methodology: R.T., S. Yoshida, S. Yonemura; Formal analysis: T.S., S. Yonemura; Investigation: T.S., S. Yonemura; Resources: R.T., S. Yoshida; Data curation: T.S.; Writing - original draft: T.S., S.T.; Writing - review & editing: S. Yoshida, S. Yonemura, S.T.; Visualization: T.S., S. Yonemura; Supervision: S.T.; Project administration: S.T.; Funding acquisition: S.T.

Funding

This work was supported by the Japan Society for the Promotion of Science through Grants-in-aid for Scientific Research (B) (JP23370094 and JP18H02454 to S.T.), Grants-in-aid for Scientific Research on Innovative Areas (JP24111002 and JP17H05782 to S.T.) and Grants-in-aid for Challenging Exploratory Research (JP17K19418 to S.T.). Additional support came from a Daiko Foundation grant of academic research on natural science (#9141 to S.T.).

Supplementary information

Supplementary information available online at
http://dev.biologists.org/lookup/doi/10.1242/dev.159343.supplemental

References

Adachi, K., Mirzadeh, Z., Sakaguchi, M., Yamashita, T., Nikolcheva, T., Gotoh, Y., Peltz, G., Gong, L., Kawase, T., Alvarez-Buylla, A. et al. (2007). Beta-catenin signaling promotes proliferation of progenitor cells in the adult mouse subventricular zone. *Stem Cells* **25**, 2827-2836.

Bänziger, C., Soldini, D., Schütt, C., Zipperlen, P., Hausmann, G. and Basler, K. (2006). Wntless, a conserved membrane protein dedicated to the secretion of Wnt proteins from signaling cells. *Cell* **125**, 509-522.

Bartscherer, K., Pelte, N., Ingelfinger, D. and Boutros, M. (2006). Secretion of Wnt ligands requires Evi, a conserved transmembrane protein. *Cell* **125**, 523-533.

Böhme, G. (1988). Formation of the central canal and dorsal glial septum in the spinal cord of the domestic cat. *J. Anat.* **159**, 37-47.

Bowman, A. N., van Amerongen, R., Palmer, T. D. and Nusse, R. (2013). Lineage tracing with Axin2 reveals distinct developmental and adult populations of Wnt/β-catenin-responsive neural stem cells. *Proc. Natl Acad. Sci. USA* **110**, 7324-7329.

Carpenter, A. C., Rao, S., Wells, J. M., Campbell, K. and Lang, R. A. (2010). Generation of mice with a conditional null allele for Wntless. *Genesis* **48**, 554-558.

Chenn, A. and Walsh, C. A. (2002). Regulation of cerebral cortical size by control of cell cycle exit in neural precursors. *Science* **297**, 365-369.

Chizhikov, V. V. and Millen, K. J. (2004). Mech.anisms of roof plate formation in the vertebrate CNS. *Nat. Rev. Neurosci.* **5**, 808-812.

Chizhikov, V. V. and Millen, K. J. (2005). Roof plate-dependent patterning of the vertebrate dorsal central nervous system. *Dev. Biol.* **277**, 287-295.

Danielian, P. S., Muccino, D., Rowitch, D. H., Michael, S. K. and McMahon, A. P. (1998). Modification of gene activity in mouse embryos in utero by a tamoxifen-inducible form of Cre recombinase. *Curr. Biol.* **8**, 1323-1326.

Goodman, R. M., Thombre, S., Firtina, Z., Gray, D., Betts, D., Roebuck, J., Spana, E. P. and Selva, E. M. (2006). Sprinter: a novel transmembrane protein required for Wg secretion and signaling. *Development* **133**, 4901-4911.

Habib, N., Li, Y., Heidenreich, M., Swiech, L., Avraham-Davidi, I., Trombetta, J. J., Hession, C., Zhang, F. and Regev, A. (2016). Div-Seq: single-nucleus RNA-Seq reveals dynamics of rare adult newborn neurons. *Science* **353**, 925-928.

Hamilton, L. K., Truong, M. K. V., Bednarczyk, M. R., Aumont, A. and Fernandes, K. J. L. (2009). Cellular organization of the central canal ependymal zone, a niche of latent neural stem cells in the adult mammalian spinal cord. *Neuroscience* **164**, 1044-1056.

Hirabayashi, Y., Itoh, Y., Tabata, H., Nakajima, K., Akiyama, T., Masuyama, N. and Gotoh, Y. (2004). The Wnt/beta-catenin pathway directs neuronal differentiation of cortical neural precursor cells. *Development* **131**, 2791-2801.

Hsiung, F., Ramirez-Weber, F.-A., Iwaki, D. D. and Kornberg, T. B. (2005). Dependence of Drosophila wing imaginal disc cytonemes on Decapentaplegic. *Nature* **437**, 560-563.

Ikeya, M. and Takada, S. (1998). Wnt signaling from the dorsal neural tube is required for the formation of the medial dermomyotome. *Development* **125**, 4969-4976.

Ikeya, M., Lee, S. M., Johnson, J. E., McMahon, A. P. and Takada, S. (1997). Wnt signalling required for expansion of neural crest and CNS progenitors. *Nature* **389**, 966-970.

Inaba, M., Buszczak, M. and Yamashita, Y. M. (2015). Nanotubes mediate niche-stem-cell signalling in the Drosophila testis. *Nature* **523**, 329-332.

Jho, E.-H., Zhang, T., Domon, C., Joo, C.-K., Freund, J.-N. and Costantini, F. (2002). Wnt/beta-catenin/Tcf signaling induces the transcription of Axin2, a negative regulator of the signaling pathway. *Mol. Cell. Biol.* **22**, 1172-1183.

Johansson, C. B., Momma, S., Clarke, D. L., Risling, M., Lendahl, U. and Frisén, J. (1999). Identification of a neural stem cell in the adult mammalian central nervous system. *Cell* **96**, 25-34.

Kondrychyn, I., Teh, C., Sin, M. and Korzh, V. (2013). Stretching morphogenesis of the roof plate and formation of the central canal. *PLoS ONE* **8**, e56219.

Kuwabara, T., Hsieh, J., Muotri, A., Yeo, G., Warashina, M., Lie, D. C., Moore, L., Nakashima, K., Asashima, M. and Gage, F. H. (2009). Wnt-mediated activation of NeuroD1 and retro-elements during adult neurogenesis. *Nat. Neurosci.* **12**, 1097-1105.

Lakso, M., Pichel, J. G., Gorman, J. R., Sauer, B., Okamoto, Y., Lee, E., Alt, F. W. and Westphal, H. (1996). Efficient in vivo manipulation of mouse genomic sequences at the zygote stage. *Proc. Natl Acad. Sci. USA* **93**, 5860-5865.

Lee, K. J. and Jessell, T. M. (1999). The specification of dorsal cell fates in the vertebrate central nervous system. *Annu. Rev. Neurosci.* **22**, 261-294.

Lee, K. J., Dietrich, P. and Jessell, T. M. (2000). Genetic ablation reveals that the roof plate is essential for dorsal interneuron specification. *Nature* **403**, 734-740.

Lie, D.-C., Colamarino, S. A., Song, H.-J., Désiré, L., Mira, H., Consiglio, A., Lein, E. S., Jessberger, S., Lansford, H., Dearie, A. R. et al. (2005). Wnt signalling regulates adult hippocampal neurogenesis. *Nature* **437**, 1370-1375.

Lois, C. and Alvarez-buylla, A. (1993). Proliferating subventricular zone cells in the adult mammalian forebrain can differentiate into neurons and glia. *Proc. Natl Acad. Sci. USA* **90**, 2074-2077.

Machon, O., Backman, M., Machonova, O., Kozmik, Z., Vacik, T., Andersen, L. and Krauss, S. (2007). A dynamic gradient of Wnt signaling controls initiation of neurogenesis in the mammalian cortex and cellular specification in the hippocampus. *Dev. Biol.* **311**, 223-237.

Madisen, L., Zwingman, T. A., Sunkin, S. M., Oh, S. W., Zariwala, H. A., Gu, H., Ng, L. L., Palmiter, R. D., Hawrylycz, M. J., Jones, A. R. et al. (2009). A robust and high-throughput Cre reporting and characterization system for the whole mouse brain. *Nat. Neurosci.* **13**, 133-140.

Maretto, S., Cordenonsi, M., Dupont, S., Braghetta, P., Broccoli, V., Hassan, A. B., Volpin, D., Bressan, G. M. and Piccolo, S. (2003). Mapping Wnt/β-catenin signaling during mouse development and in colorectal tumors. *Proc. Natl Acad. Sci. USA* **100**, 3299-3304.

Martens, D. J., Seaberg, R. M. and van der Kooy, D. (2002). In vivo infusions of exogenous growth factors into the fourth ventricle of the adult mouse brain increase the proliferation of neural progenitors around the fourth ventricle and the central canal of the spinal cord. *Eur. J. Neurosci.* **16**, 1045-1057.

McMahon, A. P. and Bradley, A. (1990). The Wnt-1 (int-1) proto-oncogene is required for development of a large region of the mouse brain. *Cell* **62**, 1073-1085.

Meletis, K., Barnabé-Heider, F., Carlén, M., Evergren, E., Tomilin, N., Shupliakov, O. and Frisén, J. (2008). Spinal cord injury reveals multilineage differentiation of ependymal cells. *PLoS Biol.* **6**, e182.

Moriyama, A., Kii, I., Sunabori, T., Kurihara, S., Takayama, I., Shimazaki, M., Tanabe, H., Oginuma, M., Fukayama, M., Matsuzaki, Y. et al. (2007). GFP transgenic mice reveal active canonical Wnt signal in neonatal brain and in adult liver and spleen. *Genesis* **45**, 90-100.

Morshead, C. M., Reynolds, B. A., Craig, C. G., McBurney, M. W., Staines, W. A., Morassutti, D., Weiss, S. and van der Kooy, D. (1994). Neural stem cells in the adult mammalian forebrain: a relatively quiescent subpopulation of subependymal cells. *Neuron* **13**, 1071-1082.

Munji, R. N., Choe, Y., Li, G., Siegenthaler, J. A. and Pleasure, S. J. (2011). Wnt signaling regulates neuronal differentiation of cortical intermediate progenitors. *J. Neurosci.* **31**, 1676-1687.

Muroyama, Y., Fujihara, M., Ikeya, M., Kondoh, H. and Takada, S. (2002). Wnt signaling plays an essential role in neuronal specification of the dorsal spinal cord. *Genes Dev.* **16**, 548-553.

Parr, B. A., Shea, M. J., Vassileva, G. and McMahon, A. P. (1993). Mouse Wnt genes exhibit discrete domains of expression in the early embryonic CNS and limb buds. *Development* **119**, 247-261.
Piccin, D. and Morshead, C. M. (2011). Wnt signaling regulates symmetry of division of neural stem cells in the adult brain and in response to injury. *Stem Cells* **29**, 528-538.
Riccomagno, M. M., Takada, S. and Epstein, D. J. (2005). Wnt-dependent regulation of inner ear morphogenesis is balanced by the opposing and supporting roles of Shh. *Genes Dev.* **19**, 1612-1623.
Roelink, H. and Nusse, R. (1991). Expression of two members of the Wnt family during mouse development–restricted temporal and spatial patterns in the developing neural tube. *Genes. Dev.* **5**, 381-388.
Roy, S., Huang, H., Liu, S. and Kornberg, T. B. (2014). Cytoneme-mediated contact-dependent transport of the Drosophila decapentaplegic signaling protein. *Science* **343**, 1244624.
Saotome, I., Curto, M. and McClatchey, A. I. (2004). Ezrin is essential for epithelial organization and villus morphogenesis in the developing intestine. *Dev. Cell* **6**, 855-864.
Ševc, J., Daxnerová, Z. and Miklošová, M. (2009). Role of radial glia in transformation of the primitive lumen to the central canal in the developing rat spinal cord. *Cell. Mol. Neurobiol.* **29**, 927-936.
Shechter, R., Ziv, Y. and Schwartz, M. (2007). New GABAergic interneurons supported by myelin-specific T cells are formed in intact adult spinal cord. *Stem Cells* **25**, 2277-2282.
Snippert, H. J., van der Flier, L. G., Sato, T., van Es, J. H., van den Born, M., Kroon-Veenboer, C., Barker, N., Klein, A. M., van Rheenen, J., Simons, B. D. et al. (2010). Intestinal crypt homeostasis results from neutral competition between symmetrically dividing Lgr5 stem cells. *Cell* **143**, 134-144.
Stenman, J. M., Rajagopal, J., Carroll, T. J., Ishibashi, M., McMahon, J. and McMahon, A. P. (2008). Canonical Wnt signaling regulates organ-specific assembly and differentiation of CNS vasculature. *Science* **322**, 1247-1250.
Takada, S., Stark, K. L., Shea, M. J., Vassileva, G., McMahon, J. A. and McMahon, A. P. (1994). Wnt-3a regulates somites and tailbud formation in the mouse embryo. *Genes Dev.* **8**, 174-189.
Takada, R., Satomi, Y., Kurata, T., Ueno, N., Norioka, S., Kondoh, H., Takao, T. and Takada, S. (2006). Monounsaturated fatty acid modification of Wnt protein: its role in Wnt secretion. *Dev. Cell* **11**, 791-801.
Toledo, E. M., Colombres, M. and Inestrosa, N. C. (2008). Wnt signaling in neuroprotection and stem cell differentiation. *Prog. Neurobiol.* **86**, 281-296.
Varela-Nallar, L. and Inestrosa, N. C. (2013). Wnt signaling in the regulation of adult hippocampal neurogenesis. *Front. Cell Neurosci.* **7**, 100.
Weiss, S., Reynolds, B. A., Vescovi, A. L., Morshead, C., Craig, C. G. and van der Kooy, D. (1996). Is there a neural stem cell in the mammalian forebrain? *Trends Neurosci.* **19**, 387-393.
Wrobel, C. N., Mutch, C. A., Swaminathan, S., Taketo, M. M. and Chenn, A. (2007). Persistent expression of stabilized beta-catenin delays maturation of radial glial cells into intermediate progenitors. *Dev. Biol.* **309**, 285-297.
Xing, L., Anbarchian, T., Tsai, J. M., Plant, G. W. and Nusse, R. (2018). Wnt/β-catenin signaling regulates ependymal cell development and adult homeostasis. *Proc. Natl Acad. Sci. USA* **115**, E5954-E5962.
Yu, K., McGlynn, S. and Matise, M. P. (2013). Floor plate-derived sonic hedgehog regulates glial and ependymal cell fates in the developing spinal cord. *Development* **140**, 1594-1604.
Zervas, M., Millet, S., Ahn, S. and Joyner, A. L. (2004). Cell behaviors and genetic lineages of the mesencephalon and rhombomere 1. *Neuron* **43**, 345-357.

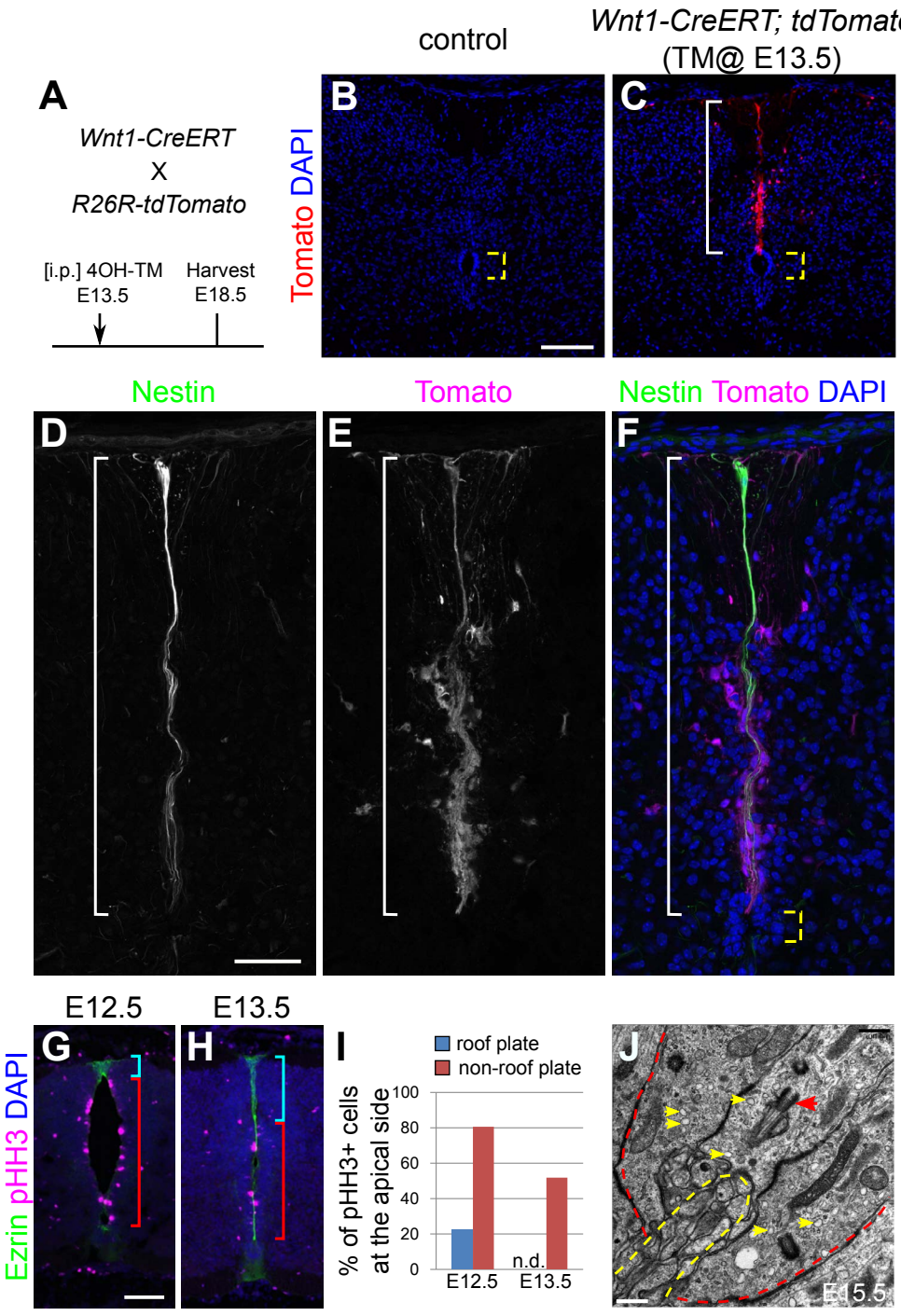

Fig. S1. Characteristics of stretched roof-plate cells. (A-F) Distribution of the progeny of roof-plate cells labeled on E13.5. A schematic diagram of labeling of roof-plate cells is shown in “A.” Transverse sections at the forelimb level of E18.5 embryos were stained with anti-RFP (B, C, E, and F) and anti-nestin antibodies (D, F). A merged image of “D” and “E” is also shown in "F". Nuclei were counterstained with DAPI (B, C, and F). Progeny of roof-plate cells labeled with tdTomato were specifically localized only along the midline of the spinal cord on E18.5 in *Wnt1-CreERT*-expressing embryos (C) but not in ittermate controls, which lacked *Wnt1-creERT* (B). Most of the nestin-positive midline cells (D) were co-present with progeny of roof-plate cells (E; Tomato). Co-staining of these tdTomato-positive cells with anti-nestin antibody revealed that the roof-plate progeny constituted 92.5% of the nestin-positive midline cells (197 of 213 nestin-positive cells). Stretched roof-plate cells are indicated by white brackets. Yellow dashed brackets indicate the lumen of the spinal cord. Scale bars: 100 μm (B), 50 μm (D). Three embryos were examined for each genotype shown in “B” and “C.” Three embryos were also examined in the analyses shown in “D”-“F”. (G-I) Proliferation on the apical side of stretched roof-plate cells and other neural epithelial cells. Transverse sections at the forelimb level are indicated. Mitotic cells were labeled with anti-phospho histone H3 (pHH3) antibody on E12.5 (G) and E13.5 (H). Roof plate was stained with anti-ezrin antibody. Nuclei were counterstained with DAPI (G, H). Ratios (as percentages) of apically dividing pHH3-positive cells to total pHH3-positive cells are indicated in “I.” While most of the neural epithelial cells divided on the apical side in both stages, roof-plate cells rarely divided during or after stretching, suggesting that stretching is distinct from typical interkinetic movement of the neural epithelial cells. Regions of the roof plate and non–roof plate are indicated by blue and red brackets, respectively. “n.d.” indicates “not detected.” Scale bar: 100 μm (G). Three embryos were examined at each stage. Twelve sections were used for the statistical analyses at each stage. (J) EM image of the tips of stretched roof-plate cells in a wild-type embryo. A basal body was observed in some sections (red arrow), and small vesicles were specifically detected at the tips of the roof-plate cells (yellow arrows). Roof-plate cells are indicated by red dashed lines. Yellow dashed line indicates the edge of the lumen of the spinal cord. Scale bar: 0.5 μm (J). Two embryos were examined.

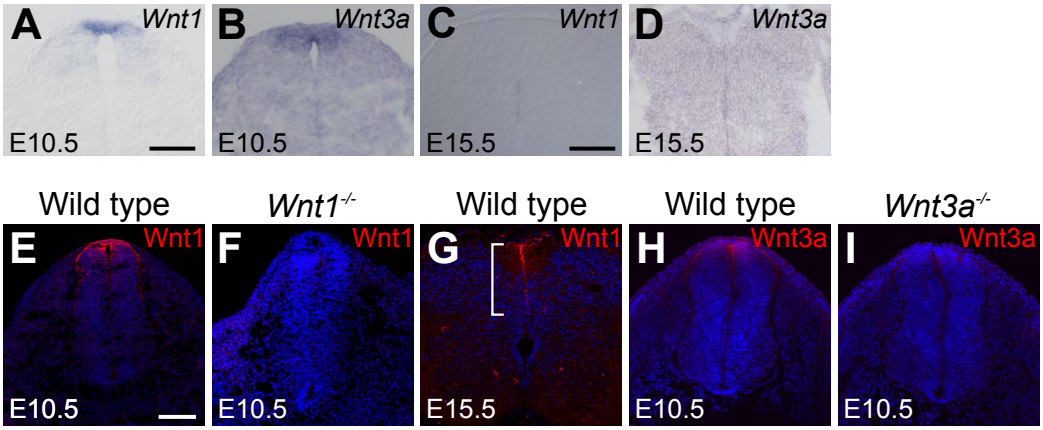

Fig. S2. Analysis of Wnt1 and Wnt3a expression in the spinal cord of mouse embryos. (A-D) *In situ* hybridization of *Wnt1* (A, C) and *Wnt3a* (B, D) on E10.5 (A, B) and E15.5 (C, D). *Wnt1* and *Wnt3a* signals could not be clearly detected by *in situ* hybridization on E15.5. (E-I) Localization of endogenous Wnt1 and Wnt3a proteins in the developing spinal cord. Immunohistochemistry was performed with dorsal spinal cords taken from *Wnt1* homozygous mutant embryos (F) and wild-type embryos (E, G) on E10.5 (E, F) and E15.5 (G) using an anti-Wnt1 antibody. Immunohistochemistry was also performed on dorsal spinal cords of *Wnt3a* homozygous mutant embryos (I) and embryos of wild-type littermates (H) on E10.5 using an anti-Wnt3a antibody. Wnt proteins were not detected in *Wnt1* or *Wnt3a* homozygous mutant embryos. Nuclei were counterstained with DAPI. Stretched roof-plate is indicated by a bracket. Scale bars: 50 μm (A), 100 μm (C, E). Three embryos were examined for each genotype. Transverse sections at the forelimb level are indicated.

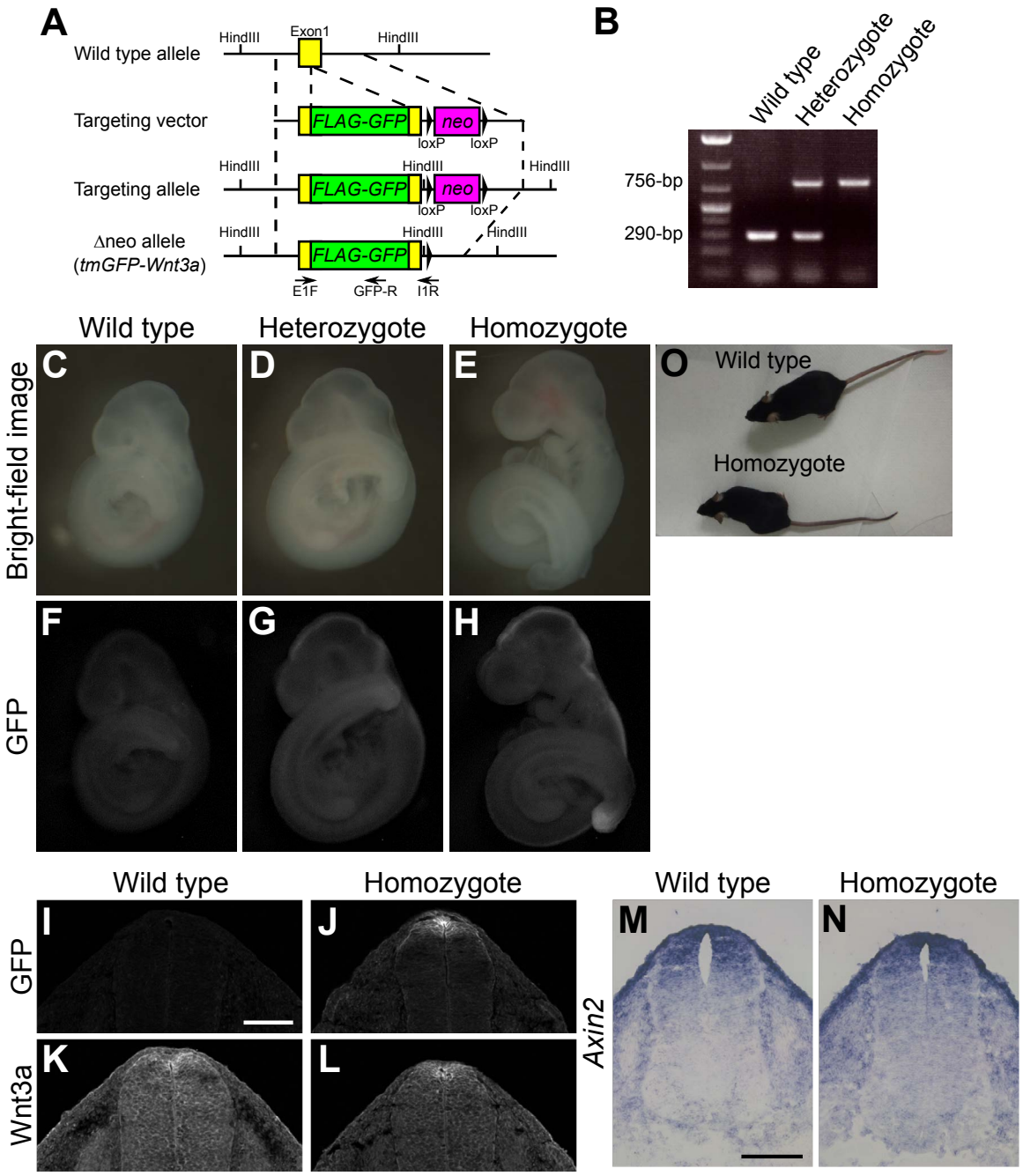

Fig. S3. Generation and analysis of *egfp-Wnt3a* knock-in mice. (A-H) Generation of the *egfp-Wnt3a* knock-in allele. Schematic representation of generation of the *egfp-Wnt3a* knock-in allele (A). We integrated FLAG-EGFP into exon 1 of *Wnt3a*, just beyond the signal peptide. The genotype of each mouse was validated by PCR analysis using the 3 primers indicated at the bottom of "A," by which a 290-bp band specific for the wild type and a 756-bp band specific for the knock-in allele were detected (B). There was no obvious difference in morphology between wild-type (C), *Wnt3a*$^{tm(GFP\text{-}Wnt3a)/+}$ (Heterozygote; D), or *Wnt3a*$^{tm(GFPWnt3a)/tm(GFP\text{-}Wnt3a)}$ (Homozygote; E) embryos on E9.5. EGFP signals in wild-type (F), *Wnt3a*$^{tm(GFP\text{-}Wnt3a)/+}$ (G), and *Wnt3a*$^{tm(GFP\text{-}Wnt3a)/tm(GFP\text{-}Wnt3a)}$ (H) embryos on E9.5 are also indicated. In "G" and "H," the EGFP signal was detected along the dorsal midline and the tailbud, consistent with the expression pattern of *Wnt3a* mRNA. Four of wild-type embryos, three of *Wnt3a*$^{tm(GFP\text{-}Wnt3a)/+}$ embryos, and two of *Wnt3a*$^{tm(GFPWnt3a)/tm(GFP\text{-}Wnt3a)}$ embryos were examined. (I-L) Comparison of localization of GFP-Wnt3a with that of endogenous Wnt3a in the dorsal spinal cord on E10.5. Transverse sections at the forelimb level are indicated. Immunohistochemical results for GFP-Wnt3a obtained with an anti-GFP antibody (I, J) and for Wnt3a using an anti-Wnt3a antibody (K, L) in a wild-type embryo (I, K) and a *Wnt3a*$^{tm(GFP\text{-}Wnt3a)/tm(GFP\text{-}Wnt3a)}$ embryo (J, L) are indicated. The distribution of the EGFP-Wnt3a signal (J) was similar to that of the endogenous Wnt3a signal (K, L). Scale bar: 100 μm (I). Three embryos were examined for each genotype. (M, N) To assess the activity of Wnt signaling, *Axin2* expression was examined by *in situ* hybridization using wild-type (M) and *Wnt3a*$^{tm(GFP\text{-}Wnt3a)/tm(GFP\text{-}Wnt3a)}$ (N) embryos. Scale bar: 100 μm (M). Three embryos were examined for each genotype. (O) *Wnt3a*$^{tm(GFP\text{-}Wnt3a)/tm(GFP\text{-}Wnt3a)}$ mice were viable and fertile.

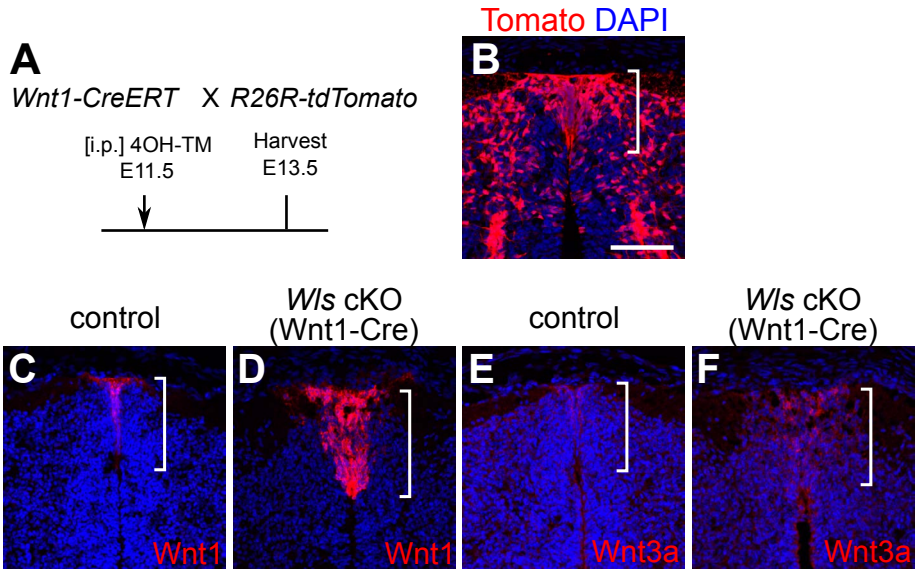

Fig. S4. Examination of the progeny of roof-plate cells suggests that unsecreted Wnt proteins remain in these cells in *Wnt1-Cre; Wls cKO* embryos. (A, B) Examination of the progeny of roof-plate cells on E13.5. Schematic diagram of labeling of roof-plate cells is shown in "A." Pregnant mice carrying these embryos were administered 4-hydroxytamoxifen (4OH-TM) 11.5 days post coitum. To detect tdTomato-positive progeny of roof plate cells, transverse sections at the forelimb level of labeled embryos on E13.5 were stained with anti-RFP antibody. Roof plate progenies stained with anti-RFP antibody are indicated. Labeled roof-plate cells examined in E13.5 embryos are indicated (B). Three embryos were examined. (C-F) Immunostaining of *Wnt1-Cre;Wls* cKO embryos (D, F) and embryos of control littermate (C, E) with anti-Wnt1 (C, D) and anti-Wnt3a (E, F) antibodies on E13.5, identical to Fig. 2"K"-"N." Note that the area where roof-plate progeny were localized in the dorsal spinal cord overlapped with that where Wnt1 and Wnt3a were detected in *Wnt1-Cre;Wls* cKO embryos on E13.5. Nuclei were counterstained with DAPI. Transverse sections at the forelimb level are indicated (B-F). Stretched roof-plate cells are indicated by brackets. Scale bar: 100 μm.

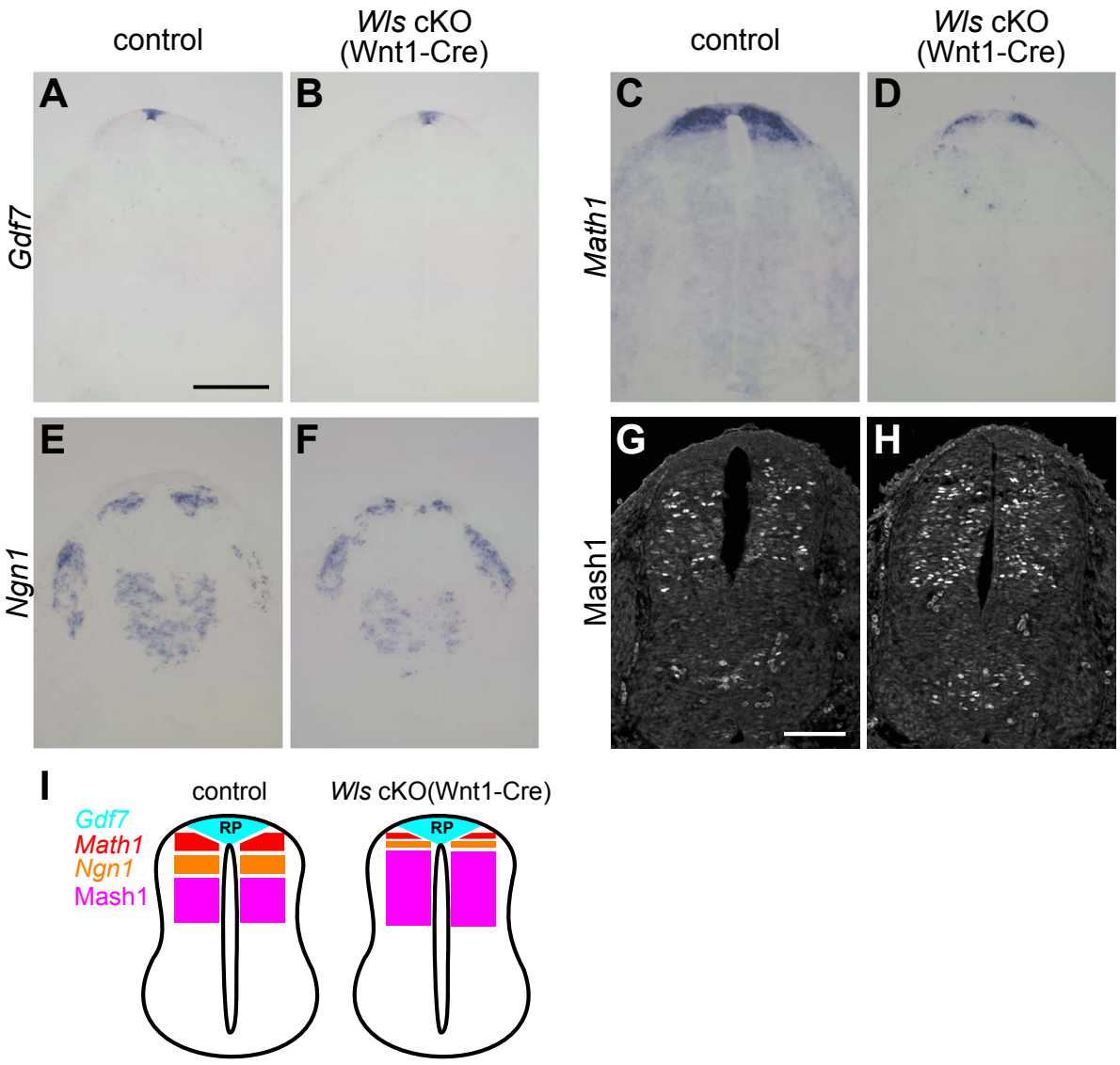

Fig. S5. The phenotype of *Wnt1-Cre;Wls* cKO embryos on E10.5. The patterning of the dorsal spinal cord was examined in *Wnt1-Cre;Wls* cKO embryos (B, D, F, H) and littermate controls (A, C, E, G) by assessing the expression of *Gdf7* mRNA (A, B; roof-plate marker), *Math1* mRNA (C, D; dI1 marker), *neurogenin (Ngn)1* mRNA (E, F; dI2 marker), and Mash1 protein (G,H; dI3-5 marker). Transverse sections at the forelimb level are indicated. As in the case of *Wnt1* and *Wnt3a* compound mutant embryos (Muroyama et al., 2002), *Math1*-positive and *Ngn1*-positive domains were reduced, whereas the Mash1-positive domain expanded. A schematic figure is shown in "I." Three embryos were examined in each experiment. Scale bars: 100 μm (A, G).

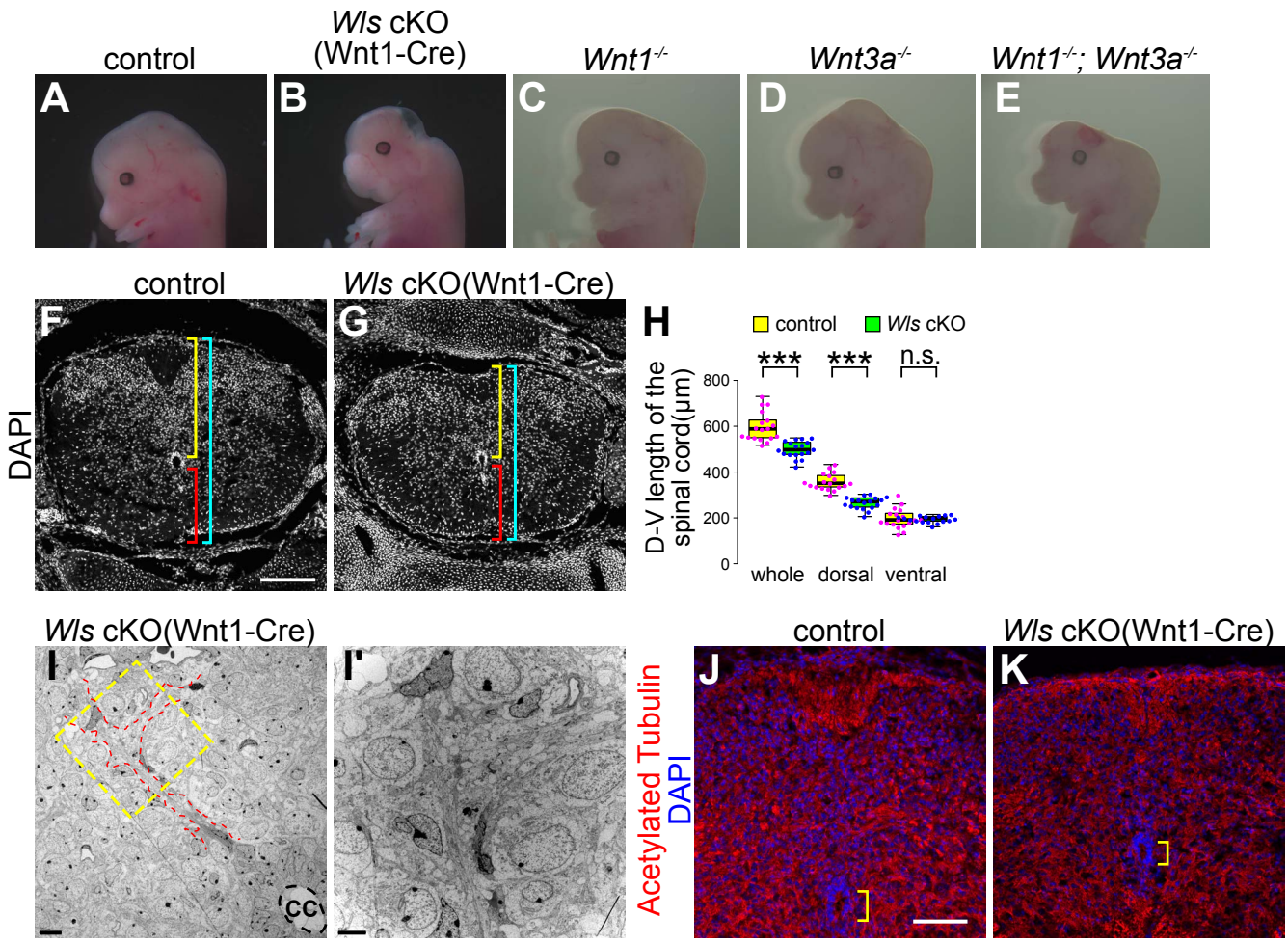

Fig. S6. Morphology of *Wnt1-Cre;Wls* cKO embryos. (A-E) Sagittal views of *Wnt1-Cre;Wls* cKO embryos on E13.5. Morphology of a *Wnt1-Cre;Wls* cKO embryo (B) and a littermate control (A) is shown. For comparison, *Wnt1* homozygous (C), *Wnt3a* homozygous (D), and *Wnt1* and *Wnt3a* compound homozygous (E) mutant embryos at the same stage are also shown. The *Wnt1-Cre;Wls* cKO embryos showed a malformed head, like the *Wnt1* and *Wnt3a* compound mutants (Muroyama et al., 2002). Two embryos were examined for each genotype. (F-H) DAPI-stained transverse section of a *Wnt1-Cre;Wls* cKO embryo (G) and a littermate control (F) on E18.5. The length of the dorsal (yellow bracket) and ventral (red bracket) regions of the spinal cord (blue bracket) was compared between *Wnt1-Cre;Wls* cKO embryos and littermate controls (H). The dorsal side was specifically reduced in size in *Wnt1-Cre;Wls* cKO embryos due to impaired proliferation caused by reduced Wnt secretion by the roof-plate cells. Scale bar: 200 μm (F). Three embryos were examined for each genotype. Eighteen sections were examined for the statistical analyses shown in "H." ***P<0.001; Student's t-test. "n.s." indicates "not significant." (I) EM images of elongated roof-plate cells. Abnormal branching of the extension in *Wnt1-Cre;Wls* cKO embryos on E18.5 (I). An enlarged image of the area marked with yellow dashed line in "I" is shown in "I'." Elongated roof-plate cells are indicated by red dashed lines. Black dashed lines indicate the edge of the lumen of the spinal cord. CC: central canal. Scale bars: 10 μm (I), 5 μm (I'). Two embryos were examined. (J, K) Immunostaining of transverse sections of *Wnt1-Cre;Wls* cKO embryos (K) and littermate controls (J) with an anti-acetylated tubulin antibody on E18.5. Nuclei were counterstained with DAPI. No obvious microtubule organization was observed in elongated roof-plate cells in either *Wnt1-Cre;Wls* cKO or littermate controls. Yellow brackets indicate the lumen of the spinal cord. Scale bar: 100 μm (J). Three embryos were examined in each experiment.

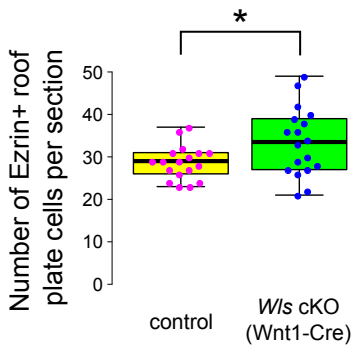

Fig. S7. Statistical analyses for ezrin-positive roof-plate cells on E13.5 (Related to Fig. 4H, I). The number of ezrin-positive roof-plate cells per section were compared between *Wnt1-Cre;Wls* cKO embryos and littermate controls on E13.5. Eighteen sections prepared from 3 embryos were examined. **P*<0.05; Student's *t*-test.

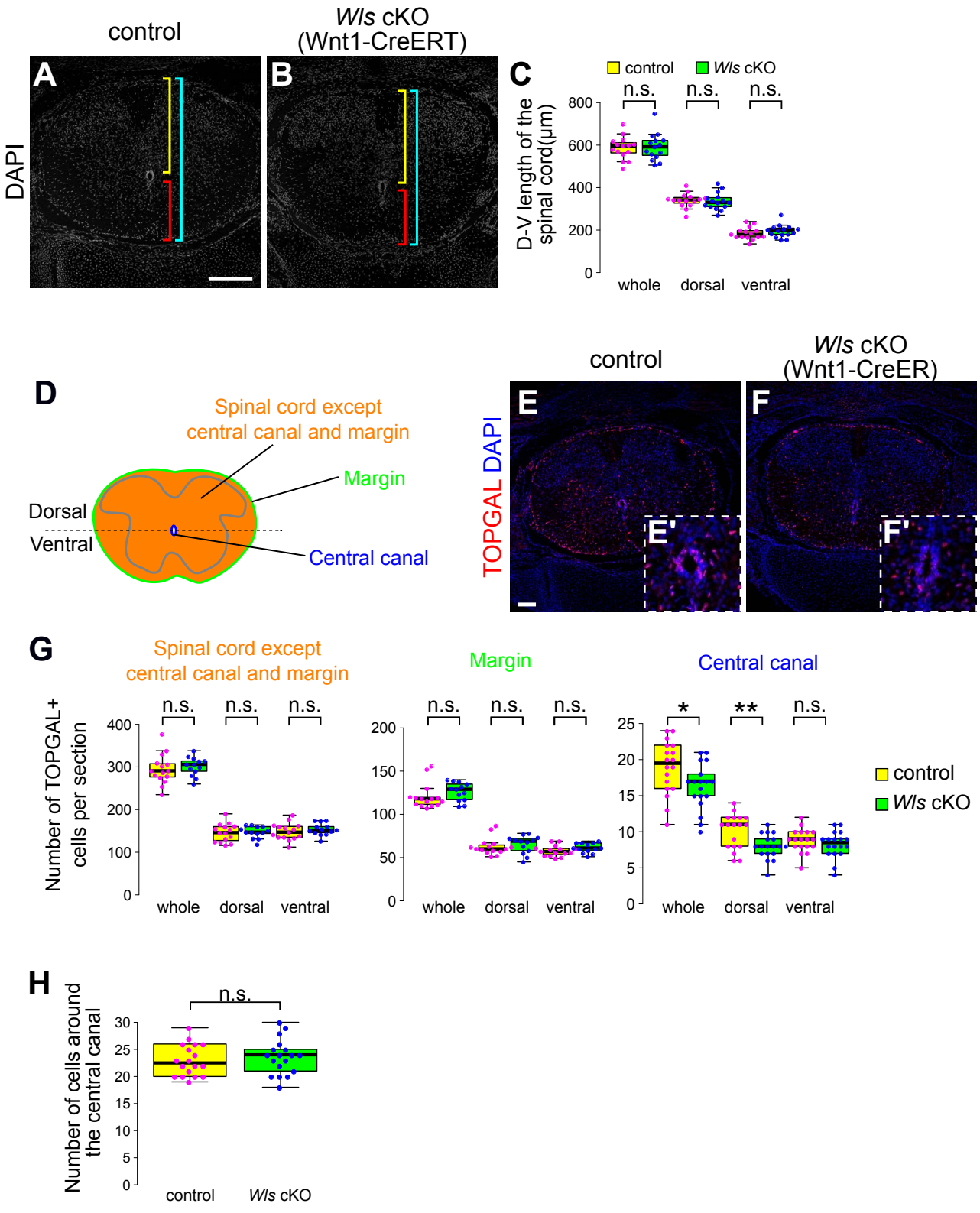

Fig. S8. Size of the spinal cord and Wnt signal activity of *Wnt1-CreERT;Wls* cKO on E18.5. (A-C) DAPI-stained Transverse section of a *Wnt1-CreERT;Wls* cKO embryo (B) and a littermate control (A) on E18.5. The size of the dorsal (yellow bracket) and ventral (red bracket) region of the spinal cord (blue bracket) was compared between *Wnt1-CreERT;Wls* cKO embryos and littermate controls (C). No obvious defect in the size of the spinal cord was observed in *Wnt1-CreERT;Wls* cKO embryos. Scale bar: 200 μm (A). Student's *t*-test. "n.s." indicates "not significant." Three embryos were examined. Fifteen sections were examined for the statistical analyses. (D-G) Schematic representation of the spinal cord (D). Wnt signaling was examined on E18.5 by using the ins-TOPGAL reporter in *Wnt1-CreERT;Wls* cKO embryos (F) and littermate controls (E) treated with 4-hydroxytamoxifen (4OH-TM) after E13.5. Transverse sections of embryos stained with anti-β-galactosidase antibody and DAPI are indicated (E, F). Magnified view of regions close to the central canal in "E" and "F" are shown in "E'" and "F'," respectively. The results of counting of TOPGAL-positive cells are indicated in (G). The average number of TOPGAL-positive cells surrounding the central canal per section is 18.9 (control) and 16.3 (*Wnt1-CreERT; Wls cKO*). Three embryos were examined in each experiment. Fifteen (control) and thirteen (*Wnt1-CreERT; Wls* cKO) sections were examined for the statistical analyses. **P* < 0.05, ***P* < 0.01; Student's *t*-test. "n.s." indicates "not significant." Note that TOPGAL signal was specifically reduced around the central canal in *Wnt1-CreERT; Wls* cKO embryos. Scale bar: 100 μm (E). (H) Statistical analyses for the number of cells surrounding the central canal in *Wnt1-CreERT;Wls* cKO mice on E18.5 (Related to Fig. 6H-J). The number of cells surrounding the central canal was not significantly different in *Wnt1-CreERT; Wls* cKO embryos on E18.5. Student's *t*-test. "n.s." indicates "not significant." Eighteen sections (three embryos) were examined.

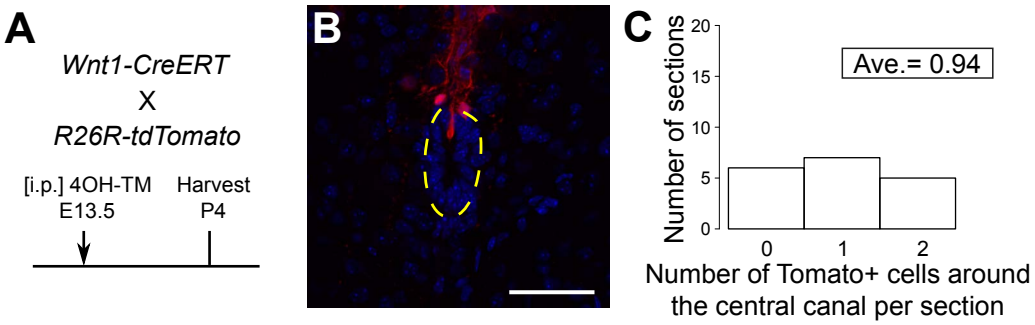

Fig. S9. Lineage tracing of roof-plate progenies from E13.5 to P4. A schematic representation is shown of lineage tracing of roof-plate cells by using P4 mice carrying *Wnt1-CreERT* and *R26R-tdTomato* (A). To detect tdTomato-positive roof-plate progenies, transverse sections of labeled mice were stained with anti-RFP antibody (B). Nuclei were counterstained with DAPI. Tomato-positive roof-plate progenies were hardly detected in the ependymal cells. Yellow dashed lines indicate the outer edge of the ependymal cells. Scale bar: 50 μm. A statistical summary is shown in "C." The number shown in the box indicates the average number of tdTomato-positive cells per section (C). Eighteen sections (3 embryos) were examined.

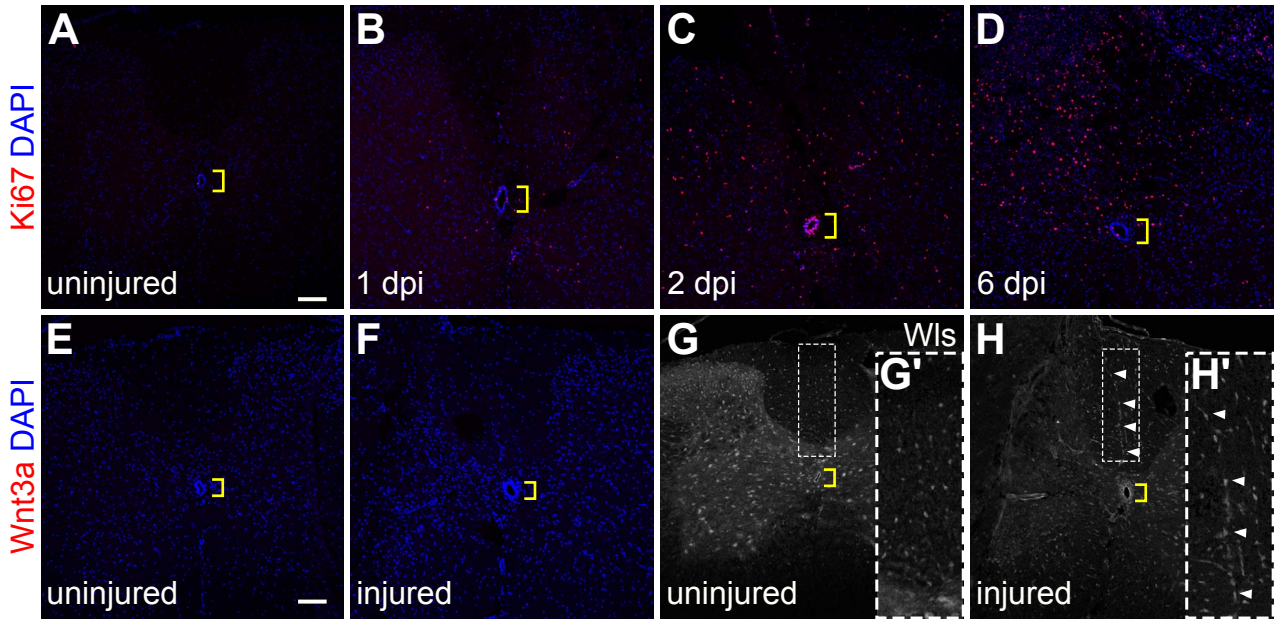

Fig. S10. Temporal change in proliferation of ependymal cells after spinal cord injury. (A-D) Immunohistochemical analysis of Ki67-positive proliferating cells of the spinal cord in uninjured mice at 8 weeks after birth (A) and 1 (B), 2 (C), or 6 (D) days post injury (dpi). The proliferation of ependymal cells was generally activated by 2 dpi. Scale bar: 100 μm (A). Two mice were examined on each day. (E-H) Expression of Wnt3a and Wls after spinal cord injury was examined by immunohistochemistry. Wnt3a expression was not detected in either uninjured (E) or injured (F) mice at 8 weeks after birth. Wls expression was detected in the dorsal midline of the spinal cord of injured mice (closed arrowheads; H) but not in that of the uninjured (G) mice. Enlarged images of the area marked by dashed lines in “G” and “H” are shown in “G’” and “H’,” respectively. Transverse sections are indicated. Scale bar: 100 μm (E). Three mice were examined in each experiment. Nuclei were counterstained with DAPI. Yellow brackets indicate ependymal cells lining the central canal.